RATIONAL SYNTHESIS AND SPECTROSCOPIC CHARACTERIZATION OF NOVEL INDOLE DERIVATIVES WITH PROMISING ANTIMICROBIAL PROPERTIES

Parvez Khan*[1], Arvind Kumar Shrivtastav[1], Raj Bhushan Singh[1]

[1]Shambhunath Institute of Pharmacy, Paryagraj, Uttar Pradesh-211015, India

***Corresponding Author:**
Parvez Khan
Research Scholar
khanparvez7754@gmail.com, Phone No: +91- 95690 80028

ABSTRACT

Background: The emergence of multidrug-resistant pathogens has created an urgent need for novel antimicrobial agents. Indole derivatives have demonstrated significant bioactivity against a wide range of microbial strains. This study focuses on the rational synthesis, structural characterization, and antimicrobial evaluation of novel indole derivatives to address this global health challenge.

Objective: To design, synthesize, and characterize a series of indole derivatives with enhanced antimicrobial properties and evaluate their efficacy against Gram-positive and Gram-negative.

Methods: A rational drug design approach was employed to identify key structural modifications of the indole core to enhance antimicrobial activity. The synthesis involved multi-step reactions, including Fischer indole synthesis, N-alkylation, and electrophilic substitution, followed by purification using recrystallization and chromatographic techniques. The derivatives were characterized using Fourier-transform infrared spectroscopy (FTIR), nuclear magnetic resonance (NMR) spectroscopy, mass spectrometry (MS), and elemental analysis. Antimicrobial screening was performed using the minimum inhibitory concentration (MIC) method and zone of inhibition assays against a panel of bacterial and fungal strains.

Results: The synthesized indole derivatives demonstrated potent antimicrobial activity, with several compounds showing superior efficacy compared to standard reference drugs. Spectroscopic analysis confirmed the successful synthesis and structural integrity of the derivatives. Structure-activity relationship (SAR) analysis revealed that the presence of electron-donating and lipophilic substituents on the indole ring enhanced antimicrobial potency.

Conclusion: This study successfully synthesized and characterized novel indole derivatives with promising antimicrobial properties. The findings highlight the potential of these derivatives as effective antimicrobial agents against resistant pathogens, thereby providing a foundation for the development of next-generation antimicrobial therapeutics. Further optimization of the identified lead compounds could pave the way for clinical applications.

Keywords: Indole, Antimicrobial agents, Synthesis, Characterization, Docking, Simulation.

1. INTRODUCTION

Indole (C_8H_7N) is a naturally occurring aromatic heterocyclic compound that has garnered significant interest due to its wide range of biological activities (Smith et al., 2015). First isolated from the indigo dye in the late 19th century, indole has since been identified as a key structural motif in numerous natural products and synthetic compounds with therapeutic potential (Jones & Wang, 2017). The indole core is present in various biologically active molecules, including alkaloids, amino acids, and pharmaceuticals (Lee et al., 2019). Its ability to interact with a variety of biological targets, including enzymes, receptors, and nucleic acids, positions indole derivatives as promising candidates in the development of new therapeutic agents (Patel et al., 2020; Kim & Choi, 2018).

Indole exhibits unique structural characteristics, including a planar geometry and electron-rich aromatic system, which contribute to its stability and reactivity (Smith et al., 2015). The nitrogen atom in the pyrrole ring can engage in hydrogen bonding and coordination with metal ions, influencing the compound's chemical behavior and interaction with biological targets (Jones & Wang, 2017). Indole is known for its electrophilic substitution reactions, particularly at the 3-position of the ring (Lee et al., 2019). The reactivity of indole can be modulated through substitution at various positions, enabling the synthesis of diverse derivatives with tailored properties (Patel et al., 2020). Additionally, indole can undergo oxidation, reduction, and functionalization, further expanding the scope of its chemical applications (Kim & Choi, 2018).

The history of indole compounds is deeply rooted in the advances of 19th-century organic chemistry, beginning with their first identification in natural products and evolving through significant synthetic developments (Gribble, 1996). Indole itself was first isolated in 1866 by Adolf von Baeyer, a German chemist who discovered it as a decomposition product of indigo dye, derived from the *Indigofera* plant, widely used for its deep blue color (Sundberg, 1996). The compound’s name combines “indigo” and “oleum” (oil), marking its initial association with the decomposition of this dye in alkaline conditions (Baeyer, 1866). Understanding indole's structure was challenging; however, significant strides were made by Emil Fischer, whose work led to the identification of indole as a fused bicyclic ring, combining benzene and pyrrole units (Fischer, 1883). Fischer’s development of the Fischer indole synthesis in 1883 was a breakthrough, allowing chemists to synthesize indole and its derivatives in the lab rather than relying solely on natural sources (Trost & Brennan, 2009). This synthesis marked a foundational moment in heterocyclic chemistry and opened the door for exploring indole’s biological roles. Soon, naturally occurring indole derivatives were identified in plants, animals, and microorganisms, highlighting indole’s biological significance (da Silva et al., 2018). Key discoveries included tryptophan, an essential amino acid involved in neurotransmitter synthesis, and indole-3-acetic acid (IAA), the primary plant growth hormone auxin, critical in plant development (Bandini et al., 2011). By the early 20th century, the pharmacological potential of indole derivatives was evident, as they became central to early synthetic drugs with sedative, analgesic, and anti-inflammatory properties, such as indomethacin, a widely recognized NSAID (Liu et al., 2016). These discoveries

established indole as a versatile scaffold in medicinal chemistry and agriculture, underscoring its significance across diverse scientific fields.

Indole derivatives have shown significant antimicrobial properties against a wide range of pathogens, including bacteria, fungi, and viruses (Fernandez et al., 2019). Compounds such as indole-3-carbinol and its derivatives have demonstrated efficacy against drug-resistant strains, highlighting the potential of indoles as alternatives to conventional antibiotics (Chung et al., 2020). Numerous studies have reported the anticancer effects of indole derivatives, particularly those that target specific signaling pathways involved in tumorigenesis (Khan et al., 2021). Indole-3-carbinol, for instance, has been shown to induce apoptosis in cancer cells and inhibit tumor growth through the modulation of estrogen metabolism (Wang et al., 2022). Indole derivatives have also exhibited anti-inflammatory and analgesic properties. Compounds such as indomethacin, a non-steroidal anti-inflammatory drug (NSAID), illustrate the therapeutic potential of indole in managing pain and inflammation through the inhibition of cyclooxygenase enzymes (Pérez et al., 2017). Research has indicated that certain indole derivatives possess neuroprotective properties, making them potential candidates for the treatment of neurodegenerative diseases (López et al., 2018). Compounds like 5-hydroxyindoleacetic acid (5-HIAA) and melatonin have been studied for their ability to modulate neurotransmitter levels and reduce oxidative stress in neuronal cells (Zhang et al., 2020).

The aim of this study is to design and synthesize novel indole derivatives, thoroughly characterize their chemical structures, and evaluate their biological potential, particularly their antimicrobial activity, to identify promising pharmaceutical candidates. To achieve this, the study focuses on developing and optimizing environmentally sustainable synthetic pathways to enhance yield; employing analytical techniques such as NMR, FTIR, Mass Spectrometry, and X-ray crystallography for structural confirmation; assessing antimicrobial efficacy through both in vitro and in silico methods against various bacterial and fungal strains; analyzing structure-activity relationships (SAR) to determine functional groups responsible for enhanced bioactivity; and ultimately, proposing pharmaceutical applications based on the observed biological effects.

2. MATERIALS AND METHODS

2.1. Literature survey

The literature review was done from standard medical and pharmaceutical databases such as PubMed, Google Scholar, ScienceDirect, etc.

2.2. Procurement of chemicals, reagents, apparatus, and solvents

2.2.1. Chemicals

Dimethyl formamide, potassium carbonate, pyrrolidine, dichloromethane, phosphorus oxychloride, thionyl chloride, mesyl chloride, tosyl chloride, and zinc metal powder were procured from HiMedia Pvt. Ltd., Mumbai, India and Sigma Aldrich Pvt. Ltd., Bangalore, India.

2.2.2. Standardized solvents

Methanol, double distilled water, glacial acetic acid, and ethanol were procured from HiMedia Pvt. Ltd., Mumbai, India.

2.2.3. Apparatus

250 ml round bottomed flasks, beakers, reflux condenser, Buchner flasks, Buchner funnel, thermometer, etc.

2.3. Rational designing of compounds using molecular docking approach

The molecular docking studies were performed as per the procedure put forward by Sharma et al., 2018.

2.3.1. Preparation of Ligand

2D-sketcher module of Schrodinger Software suite 2021-2 was used to create the structures. The Maestro environment v.12.8 was used for docking analysis. Standard drugs were downloaded from PubChem library and were uploaded in the Maestro environment. LigPrep software was used to generate stereoisomers of these ligands. A maximum of 4 poses was generated for each ligand with proper protonation states at a target pH of 7.0 using the Epik ionizer. The OPLS 2005 force field was used to build tautomerized, desalted ligands while maintaining the required chiralities of the input files, and an optimized low energy 3D ligand was created. The method addressed the docking issue using flexible ligands and moveable protein atoms.

2.3.2. Preparation of Protein

Multiple 3D crystalline target structures were downloaded from the Protein Data Bank (PDB): Crystal Structure of *E. coli* Topoisomerase-IV co-complexed with inhibitor; https://doi.org/10.2210/pdb3FV5/pdb (PDB ID: 3FV5). The target was created by removing all water molecules beyond 5A°, assigning disulfide links, bond order, and formal charges, and removing metal ions, co-factors, and heterogroup from the useable preprocessed and studied structure. With the assistance of the H-bond assignment technique, the hydrogen atoms as well as the hydrogen-bonding network was optimized. Molecular docking was used to estimate receptor grids for protein targets where the ligand would mix within the predicted active site. The grids (cubic boxes with defined dimensions) encompass the whole ligand and were built at the ligand's centroid (crystallized with the target structure). The grid box size

was increased to 126 A°, 126 A° and 126 A° (x, y, and z, respectively) to include all of the amino acid residues present in stiff macromolecules. The grid points were 0.375° apart. The Van der Waals scale factor was set to 1.0, while the charge cutoff was set at 0.25. Induced-fit docking (IFD) was conducted on each ligand, and the lowest resulting score for the best-docked posture was confirmed.

2.3.3. Induced-Fit Molecular Docking (IFD)

The IFD was created utilizing the structure-based drug design technique, which involves rendering precise geometry ligands to dock with a biological target's defined structure. The free-state ligands were docked into the rigid state receptor's active site, enzyme, tube, etc., resulting in a predicted binding mode and the strength of the fit being evaluated. In receptor-based computational techniques, the attachment of a low-molecular-weight ligand to a macromolecular protein has its own significance since the most suitable connection with low energy values and possible steric conflicts is found. During the docking process, a maximum of 10 conformers was evaluated. The population was limited to 150 individuals, which was selected at random. The mutation rate was set to 0.02 and the crossover rate was set to 0.8. The maximum number of energy evaluations was set to 500000, the maximum number of generations was set to 1000, the maximum number of top individuals that automatically survived was set to 1. Translations were a 0.2 step size, quaternions were a 5.0° step size, and torsions was a 5.0° step size. Cluster tolerance was set to 0.5, external grid energy to 1000.0, maximum binding energy to 0.0, maximum number of retries to 10000, and 10 LGA runs was performed. The interactions and binding energy of the docked structure was studied. It was performed many times to get different docked conformations as well as to assess anticipated docking energy. The optimal ligand-receptor structure was selected among the docked structures based on the ligand's lowest energy and minimum solvent accessibility. The compounds were rated based on the information gathered, and a subset was examined experimentally for biological activity. For each ligand, the Glide Score was calculated.

2.4. Computational studies

The computational studies were performed as per the procedure put forward by Deokar and Shaikh, 2022.

2.4.1. Pharmacokinetics, Bioavailability, and Drug-likeliness studies

The SwissADME online tool was used to conduct a prediction research of pharmacokinetics, namely ADME, bioavailability, and drug-likeness of ligands. To identify drug-likeness, the technology estimates bioavailability radar based on six physicochemical properties: lipophilicity, size, polarity, insolubility, flexibility, and insaturation. The ADME properties, such as passive human gastrointestinal absorption (HIA) and blood-brain barrier (BBB) permeation, as well as substrate or non-substrate of the permeability glycoprotein (P-gp) was detected positive or negative in the BOILED-Egg model within the tool. The lipophilicity estimation (Log p/w) parameters such as iLOGP on free energies of solvation in n-octanol

and water calculated by the generalized-born and solvent accessible surface area (GB/SA) model, XLOGP3 is an atomistic method with corrective factors and a knowledge-based library, WLOGP is an implementation of a purely atomistic method, and MLOGP is an archetype of topological method rely. The Lipinski (Pfizer) filter, which is the first rule-of-five to be implemented in a tool, was used to predict drug-likeness. The bioavailability radar was used to predict oral bioavailability based on several physicochemical characteristics. The ranges of each parameter was mentioned as LIPO = lipophilicity as -0.7 < XLOGP3 < +5.0; SIZE = size as molecular weight 150gm/mol < MV < 500gm/mol; POLAR = polarity as 20Å² < TPSA (topological polar surface area) < 130Å²; INSOLU = insoluble in water by log S scale 0 < Logs (ESOL) < 6; INSATU = insaturation or saturation as per fraction of carbons in the sp3 hybridization 0.3 < Fraction Csp3 < 1 and FLEX = flexibility as per rotatable bonds 0 < Number of rotatable bonds < 9.

2.4.2. Drug Target Identifications

SwissTargetPrediction is a web service for bioactive small molecule target prediction. This website enables to anticipate a tiny molecule's targets. It compares the query molecule to a library of 280,000 molecules active on more than 2000 targets in five distinct species using a mix of 2D and 3D similarity metrics. Understanding the molecular processes behind bioactivity and anticipating possible side effects or cross-reactivity requires mapping the targets of bioactive small compounds. Predictions have been made in three distinct organisms (models), and for near paralogs and orthologs, mapping predictions by homology within and across species is possible. The human (*Homo sapiens*), rat (*Rattus norvegicus*), and mouse (*Mus musculus*) models have all been shown to have credible inhibitory targets for the ligands.

2.4.3. Core scaffold-based bioisosteric search

The SwissBioisostere database contains information on molecular replacements and their performance in biochemical assays. It is meant to provide researchers in drug discovery projects with ideas for bioisosteric modifications of their current lead molecule, as well as to give interested scientists access to the details on particular molecular replacements. Ligands' core scaffold was studied comprehensively through bioisosteric replacements to produce various heterocycles (tetrahydropyran, pyridine, pyrrole, pyrazole, pyrimidine, piperidine, morpholine, piperazine, etc.). The parameters affecting the biological target and associated activities was taken into account and the derived data was interpreted.

2.5. Selection of most active series of compounds for practical synthesis

The compounds showing the best Glide scores, completely following the Lipinski's rule of five, have optimized pharmacokinetic profile, and depicting affinity towards particular molecular targets was selected for practical synthesis.

2.6. Molecular simulation study of the most promising compound using Gromacs® software

The molecular dynamics simulation of the ligand was done using the GROMACS simulation Package and CHARMM 27 force field. To obtain the molecular topology file compatible with the CHARMM 27 force field, SwissParam web service was utilized to explicit water model, the protein-ligand assembly was solvated and the completely system was neutralized with the addition of Na ions by replacing the water molecules. After completing these steps, the energy minimization of the system was done, which was followed by equilibration of the system using two consecutive NVT (5 ns) and NPT (5 ns) runs. To fix all NVT and NPT runs, the V-rescale thermostat and Berendsen barostat for temperature (298 K) and pressure (1 bar) were used, respectively. Finally, the resulting ensembles were introduced to 40ns MD simulation with a time-stage of 2 fs for each simulation. Cut-off ratios of 1 nm and smooth Particle Mesh Ewald (PME) protocol was used for treat the long-range electrostatic interactions The snapshots of simulation trajectories was observed using visual molecular dynamics (VMD) software. Root mean square deviation (RMSD) of peptide (atom backbone), radius of gyration (Rg) and root-mean-square fluctuation (RMSF) values was plotted using XMGRACE.

2.7. Synthesis of indole molecule

To synthesize a novel indole derivative (4-(3-methylbut-2-en-1-yl)-1-tosyl-1*H*-indole) starting from 1-bromo-2-methyl-3-nitrobenzene, the process begins with the reduction of the nitro group to an amine. The 1-bromo-2-methyl-3-nitrobenzene was dissolved in ethanol and treated with sodium hydroxide, followed by heating under reflux conditions for several hours. The progress of the reaction was monitored using thin-layer chromatography (TLC) until the nitro group is fully reduced to an amine. Once the reduction is complete, the resulting aniline derivative was subjected to cyclization to form the indole ring. This was achieved by adding the aniline product to a mixture of formic acid and ammonium acetate in a round-bottom flask, which was then heated under reflux for duration of 3 to 6 hours. During this reaction, the aniline reacts with formic acid, facilitating the formation of the indole structure. After the cyclization step, the reaction mixture was allowed to cool, and acetic acid is gradually added to quench any remaining reactants. The pH of the mixture was adjusted to neutral using sodium hydroxide, followed by extraction of the product with an appropriate organic solvent, such as dichloromethane or ethyl acetate. The organic layer was then dried over anhydrous magnesium sulfate to remove any residual water, and the solvent is removed using a rotary evaporator, yielding a crude indole derivative. The crude product was purified through column chromatography or recrystallization based on solubility to obtain the final product. Finally, characterization of the synthesized indole derivative was performed using various analytical techniques, including NMR spectroscopy and mass spectrometry, to confirm the successful formation of the desired compound (**Figure 5.1**).

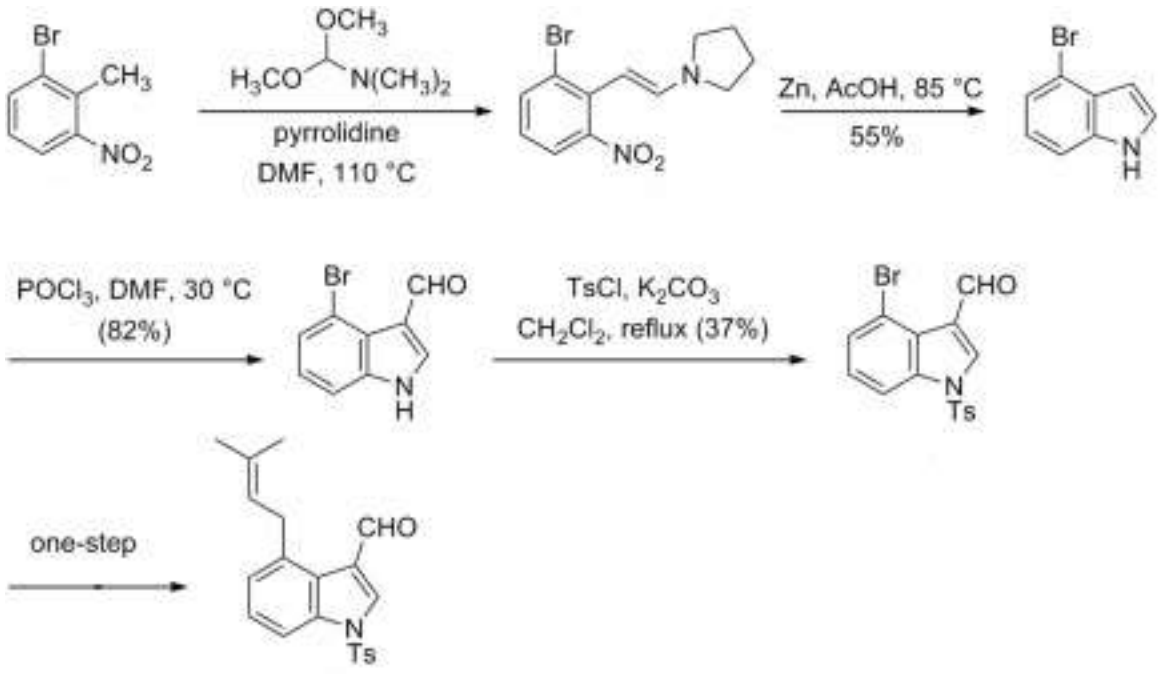

Figure 5.1. Synthesis of novel Indole derivatives.

Reaction mechanism:

The synthesis of 4-(3-methylbut-2-en-1-yl)-1-tosyl-1*H*-indole from 1-bromo-2-methyl-3-nitrobenzene can be achieved through a series of key reaction steps. Each step involves crucial transformations to introduce the indole system, tosyl protection, and prenylation of the indole nucleus.

Step 1: Reduction of Nitro Group to Amine

Reagent: Fe/Acetic Acid (or Sn/HCl)

Reaction Type: Reduction

Mechanism:

1. The 1-bromo-2-methyl-3-nitrobenzene is reduced to 1-bromo-2-methyl-3-aminobenzene.
2. The nitro group ($–NO_2$) is converted to an amino group ($–NH_2$) via a multi-electron transfer mechanism facilitated by iron filings (Fe) in acetic acid or tin (Sn) in the presence of hydrochloric acid (HCl).

Reaction:

1-Bromo-2-Methyl-3-Nitrobenzene → 1-Bromo-2-Methyl-3-Aminobenzene

Step 2: Cyclization to Form Indole Core (Fischer Indole Synthesis)

Reagent: Ethyl Formate / Formic Acid (HCOOH)

Reaction Type: Fischer Indole Synthesis

Mechanism:

1. The 1-bromo-2-methyl-3-aminobenzene undergoes cyclization with ethyl formate (or formic acid) to form the corresponding indole structure.
2. The reaction proceeds via nucleophilic attack of the amino group ($-NH_2$) on the carbonyl carbon of formic acid, leading to an imine intermediate.
3. Rearrangement and cyclization occur to form the 1-bromo-2-methyl-indole.

Reaction:

1-Bromo-2-Methyl-3-Aminobenzene + HCOOH → 1-Bromo-2-Methyl-Indole

Step 3: *N*-Tosylation of Indole

Reagent: Tosyl Chloride (TsCl), Pyridine (Base)

Reaction Type: Nucleophilic Substitution (*N*-Tosylation)

Mechanism:

1. The 1-bromo-2-methyl-indole reacts with tosyl chloride (TsCl) in the presence of a base (like pyridine), leading to the formation of 1-tosyl-1*H*-indole.
2. The nitrogen of the indole ring (N-H) acts as a nucleophile and attacks the electrophilic sulfur atom in tosyl chloride.
3. This results in the displacement of the chloride ion (Cl^-) and formation of *N*-tosylated indole.

Reaction:

1-Bromo-2-Methyl-Indole + TsCl → 1-Tosyl-1*H*-Indole

Step 4: Metal-Halogen Exchange (Lithiation)

Reagent: n-Butyllithium (n-BuLi)

Reaction Type: Metal-Halogen Exchange

Mechanism:

1. The 1-tosyl-1*H*-indole with a bromine substituent at position 2 is treated with n-butyllithium (n-BuLi).
2. The n-BuLi induces a metal-halogen exchange at the 2-position, forming a lithium-indole intermediate.
3. The intermediate is now highly nucleophilic and ready for reaction with an electrophile.

Reaction:

1-Bromo-1-Tosyl-1*H*-Indole → 2-Lithio-1-Tosyl-1*H*-Indole

2.8. Characterization of compounds using laboratory techniques

The synthesized molecules was characterized in terms of Yield (from the formula; Practically obtained weight / Theoretically calculated weight × 100), Appearance (colour and state), Melting point (calculated using Thiele's tube method), and Retention factor (based on optimized chromatographic solvent system).

2.9. Characterization of compounds using sophisticated analytical techniques

The synthesized molecules was comprehensively characterized using sophisticated analytical techniques such as Fourier-transformed Infrared (FT-IR) Spectroscopy, Proton-Nuclear Magnetic Resonance (^{1}H-NMR) Spectroscopy, Carbon-Nuclear Magnetic Resonance (^{13}C-NMR) Spectroscopy, and Mass Spectroscopy; where specific peaks was studied to establish the chemical structures of the newly synthesized molecules. CHN-Elemental Analysis was used to determine Carbon, Hydrogen, and Nitrogen compositions (in %) in the molecules and compare with the theoretically calculated values.

2.10. Anti-bacterial activity

Modified agar well diffusion method will be used to detect the antibacterial activities of different extracts and formulations. In this method, each nutrient agar plates will be planted with 0.2 mL of 24 hr broth culture of *Staphylococcus aureus*, soybean casein digest media plates will be seeded with 0.2 mL each of 24 hr broth culture of *Staphylococcus aureus*. The plates will be dried for 1 hr. In each of the plates, equidistant wells will be excavated with a sterile 8 mm borer. Into each plate, 0.5 mL of indole solution (experimental) and clindamycin (standard drug) will be introduced. The plates of will be incubated at 37°C ± 1°C for 24 hr. The diameter of the zones of inhibition (in mm) will be measured for evaluating the antibacterial activity. The experiment will be repeated three times and the mean was recorded. Dimethyl sulfoxide (DMSO) will be employed as negative control.

2.11. Statistical analysis of the results

All the data was represented in Mean ± SD. Data was analyzed using one-way ANOVA followed by Dunnett's multiple comparison tests using Sigmastat® software. The group means was considered significantly significant when p-value is < 0.05

2.12. Compilation and analysis of data

After completion of the research work, all the data of various sections and sub-sections was compiled suitably and was analyzed statistically and logically.

2.13. Publication of results in Open Access journal

After the compilation of all the data, the results were published in any international reputed Open Access journal.

3. RESULTS AND DISCUSSION

3.1. Pharmacokinetics, Bioavailability, and Drug-likeliness studies

3.1.1. Compound-1

Table 1 describes the predictive values for pharmacokinetics, bioavailability and drug-likeness data on novel Indole derivative. The molecule-1 showed high absorption rate. Good blood-brain permeability was obtained based on LogP value while low negative value indicated less skin permeation. In case of metabolism, the molecule did not prove to be a p-glycoprotein substrate. It acts as CYP_{450} inhibitors and specifically inhibits CYP1A2 and CYP2D6 isoforms. For the prediction of bioavailability and drug-likeness, a moderate bioavailability score was obtained. Poor water soluble characteristics were obtained for the novel Indole derivative.

3.1.2. Compound-2

The molecule-2 showed high absorption rate. Good blood-brain permeability was obtained based on LogP value while moderate negative value indicated less skin permeation. In case of metabolism, the molecule did prove to be a p-glycoprotein substrate. It acts as CYP_{450} inhibitors and specifically inhibits CYP2D6 isoform. For the prediction of bioavailability and drug-likeness, a moderate bioavailability score (0.55) was obtained. Poor to moderate water soluble characteristics were obtained for this novel Indole derivative.

3.1.3. Compound-3

The molecule-3 (**Figure 1**) showed low absorption rate. Poor blood-brain permeability was obtained based on LogP value while low negative value indicated less skin permeation. In

case of metabolism, the molecule did prove to be a p-glycoprotein substrate. It acts as CYP_{450} inhibitors and specifically inhibits CYP2C19 and CYP2D6 isoforms. For the prediction of bioavailability and drug-likeness, a moderate bioavailability score (0.55) was obtained. Poor water soluble characteristics were obtained for the novel Indole derivative.

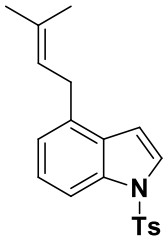

Compound-1
(Tosyl chloride)

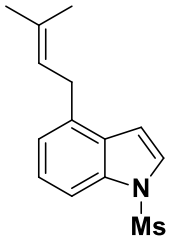

Compound-2
(Mesyl chloride)

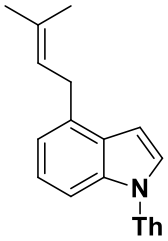

Compound-3
(Thionyl chloride)

Figure 1. Structure of novel Indole derivatives.

Table 1. Pharmacokinetics and physicochemical properties of novel Indole derivatives.

PROPERTIES	**Compound-1**	**Compound-2**	**Compound-3**
Physicochemical Properties			
Formula	$C_{26}H_{25}ClO_5S$	$C_{20}H_{21}ClO_4S$	$C_{21}H_{24}O_5S$
Molecular weight (g/mol)	484.11	392.08	388.13
Number of heavy atoms	26	27	26
Number of aromatic heavy atoms	12	12	12
Fraction Csp^3	0.48	0.50	0.50
Number of rotatable bonds	7	8	7
Number of H-bond acceptors	2	2	1
Number of H-bond donors	2	1	1
Molar Refractivity	111.71	116.18	114.65
TPSA (A^2)	35.05	24.50	15.27
SMILES	O=C(CCCCC1=CC=CC=C1)/C=C/C2=CC=C(OS(C3=CC=C(Cl)C=C3)(=O)=O)C(OC)=C2	O=C(CCCCC1=CC=CC=C1)/C=C/C2=CC=C(OS(Cl)=O)C(OC)=C2	O=C(CCCCC1=CC=CC=C1)/C=C/C2=CC=C(OS©(=O)=O)C(OC)=C2

Lipophilicity			
Log Po/w (Ilog p)	3.67	4.42	4.40
Log Po/w (XL OGP3)	5.99	6.32	6.71
Log Po/w (WL OGP)	5.53	5.84	6.14
Log Po/w (ML OGP)	4.05	4.26	4.87
Log Po/w (SIL ICOS-IT)	4.65	5.20	5.66
Consensus Log Po/w	4.78	5.21	5.56
Water Solubility			
Log S (ESOL)	-5.68	-5.90	-6.12
Solubility	7.39e-04 mg/ml ; 2.09e-06 mol/l	4.67e-04 mg/ml ; 1.27e-06 mol/l	2.66e-04 mg/ml ; 7.58e-07 mol/l
Class	Moderate Soluble	Moderate Soluble	Poorly Soluble
Log S (Ali)	-6.51	-6.62	-6.83
Solubility	1.08e-04 mg/ml ; 3.07e-07 mol/l	8.71e-05 mg/ml ; 2.38e-07 mol/l	5.13e-05 mg/ml ; 1.46e-07 mol/l
Class	Poorly Soluble	Poorly Soluble	Poorly Soluble
Log S (SILICOS-IT)	-6.83	-7.53	-7.80
Solubility	5.17e-05 mg/ml ; 1.47e-07 mol/l	1.09e-05 mg/ml ; 2.97e-08 mol/l	5.58e-06 mg/ml ; 1.59e-08 mol/l
Class	Poorly Soluble	Poorly Soluble	Poorly Soluble
Pharmacokinetics			
GI absorption	High (93.747%)	High (94.736%)	Low (83.636%)
BBB permeant	Yes (-0.942)	Yes (-0.168)	No
CNS permeability	-2.159	-2.337	-2.281
P-gp substrate	No	Yes	Yes
Caco2 permeability	0.421	1.131	0.943
CYP1A2 inhibitor	Yes	No	No
CYP2C19 inhibitor	No	No	Yes
CYP2C9 inhibitor	No	No	No
CYP2D6	Yes	Yes	Yes

inhibitor			
CYP3A4 inhibitor	No	No	No
Log Kp (skin permeation) (cm/s)	-4.20	-4.05	-3.67
Total clearance (log ml/min/kg)	-0.317	-0.106	-0.462
Renal OCT2 substrate	No	No	No
Toxicity			
Minnow toxicity (log mM)	-1.583	-1.013	-1.083
T. pyriformis toxicity (log ug/L)	0.295	1.099	1.259
Oral Rat Acute Toxicity (LD_{50}) (mol/kg)	2.349	2.577	2.667
Oral Rat Chronic Toxicity (LOAEL) (log mg/kg_bw/day)	1.17	1.287	1.374
Max. tolerated dose (human) (log mg/kg/day)	0.321	0.787	0.344
Hepatotoxicity	No	No	No
Skin Sensitisation	No	No	No
AMES toxicity	No	No	No
Drug-likeness			
Lipinski	Yes; 0 violation	Yes; 1 violation: MLOGP>4.15	Yes; 1 violation: MLOGP>4.15
Ghose	Yes	No; 1 violation: WLOGP>5.6	No; 1 violation: WLOGP>5.6
Veber	Yes	Yes	Yes

Egan	Yes	Yes	No; 1 violation: WLOGP>5.88
Muegge	No; 1 violation: XLOGP3>5	No; 1 violation: XLOGP3>5	No; 1 violation: XLOGP3>5
Bioavailability Score	0.55	0.55	0.55
Medicinal Chemistry			
PAINS	0 alert	0 alert	0 alert
Brenk	1 alert: hydroquinone	0 alert	0 alert
Lead-likeness	No; 2 violations: MW>350, XLOGP3>3.5	No; 3 violations: MW>350, Rotors>7, XLOGP3>3.5	No; 2 violations: MW>350, XLOGP3>3.5
Synthetic accessibility	3.19	3.30	3.28

3.2. Bioavailability Radar Plot

3.2.1. Compound-1

The bioavailability radar for oral bioavailability prediction showed desired INSATU = insaturation as per Csp^3 as 0.48, FLEX as per number of rotable bond 7, INSOLU Logs (ESOL) as -5.68 (insoluble), SIZE as molecular weight (g/mol) of 329.04, POLAR as TPSA ($Å^2$) 35.05, and LIPO as XLOGP3 value of 5.99 (**Figure 2A**).

3.2.2. Compound-2

The bioavailability radar for oral bioavailability prediction showed desired INSATU = insaturation as per Csp^3 as 0.50, FLEX as per number of rotable bond 8, INSOLU Logs (ESOL) as -5.90 (insoluble), SIZE as molecular weight (g/mol) of 366.54, POLAR as TPSA ($Å^2$) 24.50, and LIPO as XLOGP3 value of 6.32 (**Figure 2B**).

3.2.3. Compound-3

The bioavailability radar for oral bioavailability prediction showed desired INSATU = insaturation as per Csp^3 as 0.50, FLEX as per number of rotable bond 7, INSOLU Logs (ESOL) as -6.12 (insoluble), SIZE as molecular weight (g/mol) of 350.54, POLAR as TPSA ($Å^2$) 15.27, and LIPO as XLOGP3 value of 6.71 (**Figure 2C**).

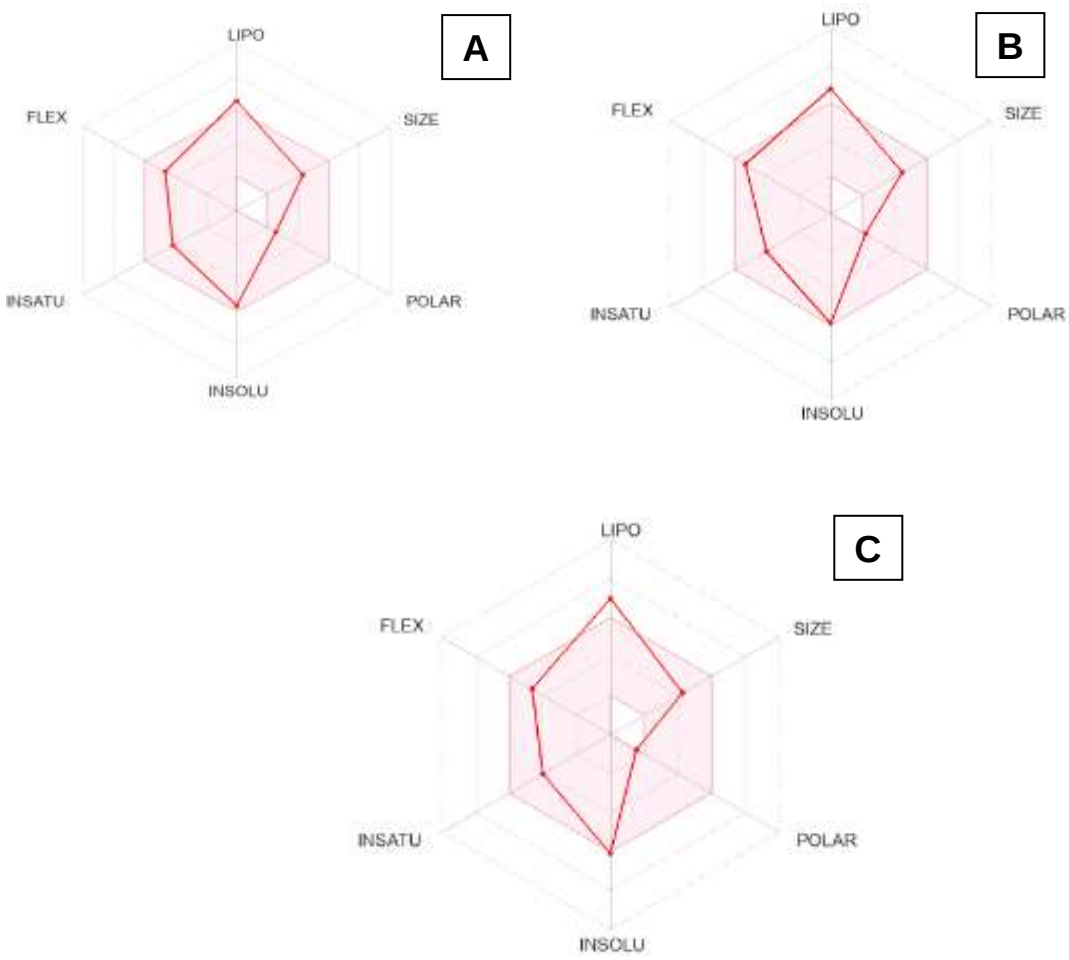

Figure 2. Bioavailability Radar Plot (A) Compound-1, (B) Compound-2, and (C) Compound-3.

3.3. Boiled Egg Plot

In case of BOILED-Egg model (**Figure 3**), the Brain OrIntestinaLEstimateD permeation method (BOILED-Egg) has already been proposed as an accurate predictive model, which helps by computational prediction of the lipophilicity and polarity of small molecules. In overall predictive results, novel Indole derivative can be suitable drug candidate as per bioavailability radar and BOILED-Egg representation.

3.3.1. Compound-1

It was observed in the predictions that compound-1 (**Figure 3A**) was a PGP positive non-substrate. PGP positive non-substrate molecules are compounds that interact with P-glycoprotein but are not themselves transported by it. These molecules can influence PGP activity in several ways, such as inhibiting or activating its transport function, altering its expression levels, or modulating its conformation. Unlike substrates that are actively pumped out of cells by PGP, non-substrate molecules bind to PGP and affect its function without being expelled.

3.3.2. Compound-2

It was obtained that novel Indole derivative, compound-2 (**Figure 3B**) has limited capability of blood-brain barrier penetration as well as it also showed low gastrointestinal absorption. The molecule was found to be PGP positive as non-substrate in predictive model.

3.3.3. Compound-3

PGP positive non-substrate behaviour was observed in the predictions for compound-3 (**Figure 3C**). PGP positive non-substrate molecules represent a significant area of interest in pharmacology and drug development. By modulating the function and expression of P-glycoprotein, these molecules offer potential strategies for overcoming multidrug resistance, optimizing drug pharmacokinetics, and enhancing therapeutic efficacy. Ongoing research continues to explore and develop new PGP inhibitors and modulators, aiming to address the challenges posed by drug resistance and improve patient outcomes across various medical conditions.

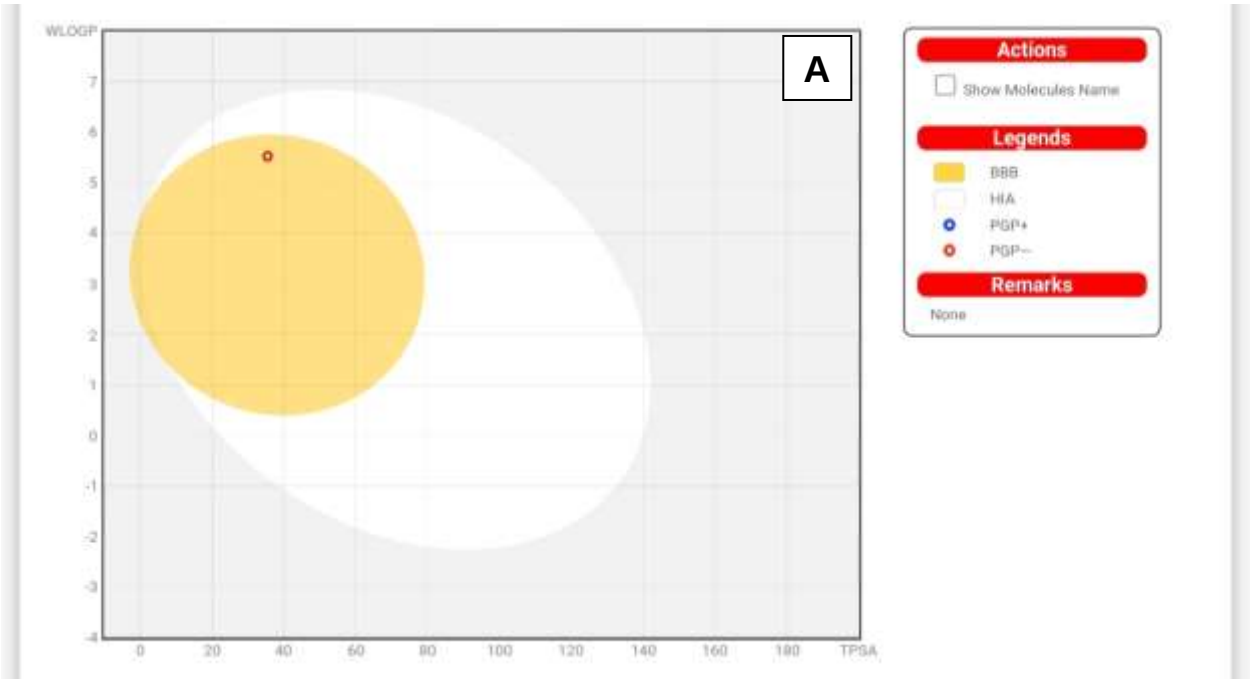

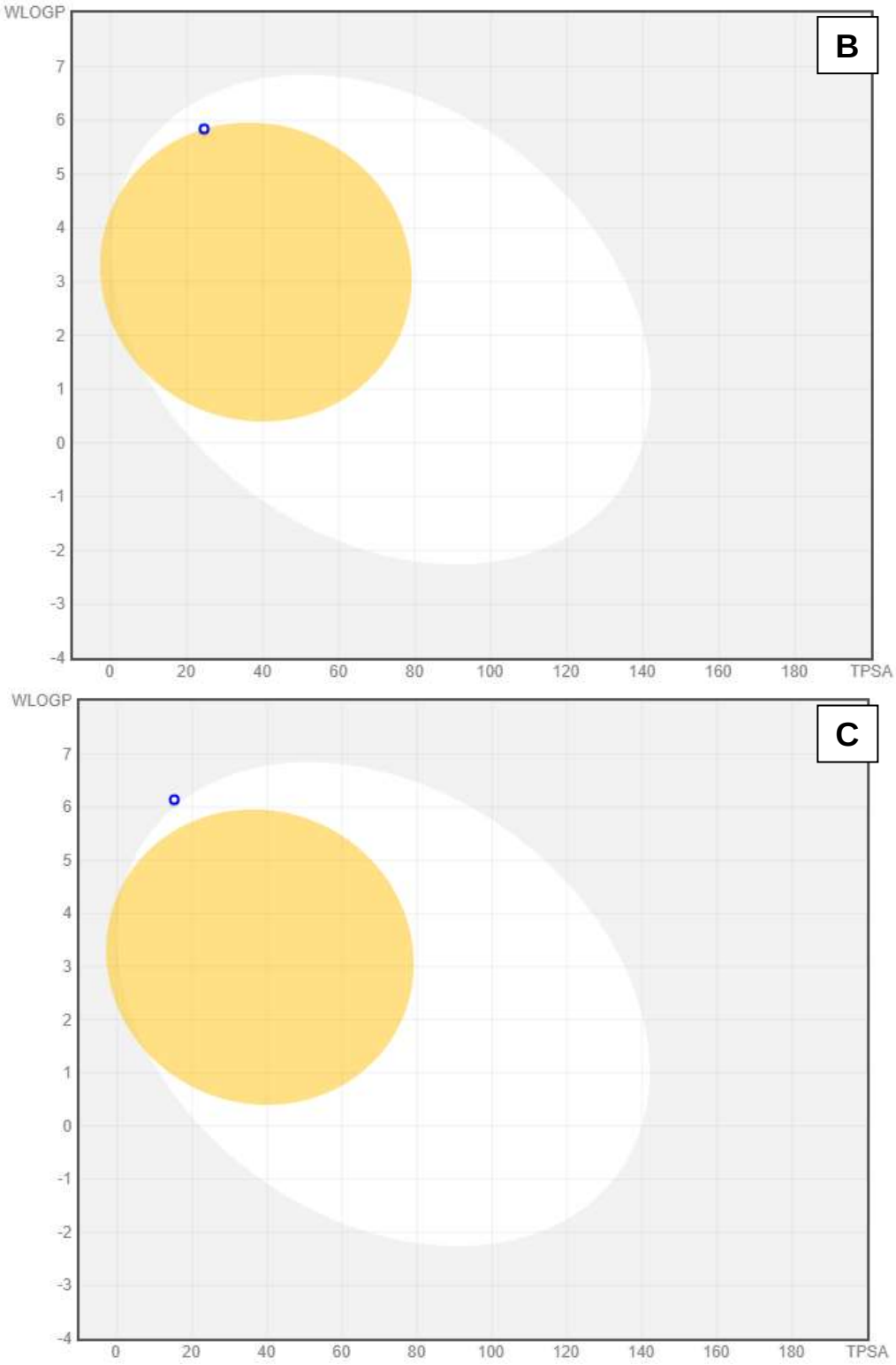

Figure 3. Boiled Egg Plot (A) Compound-1, (B) Compound-2, and (C) Compound-3.

3.4. Drug target identification

3.4.1. Compound-1

As the study is focused on drug repurposing, it remains crucial to determine the plausible therapeutic targets against which Compound-1 can inhibit them with micromolar concentrations, ideally. The human (*Homo sapiens*), rat (*Rattus norvegicus*), and mouse (*Mus musculus*) models revealed the inhibitory perspectives of compound-1 against several targets like hydrolase, enzyme, oxidoreductase, Family A G protein-coupled receptor, transferase, voltage-gated ion channel, primary active transporter, ligand-gated ion channel, etc. (**Figure 4**). The predicted results strongly supported the basis of indoles for possible applications against antimicrobial targets by revealing the possibilities of drug interactions with multiple targets.

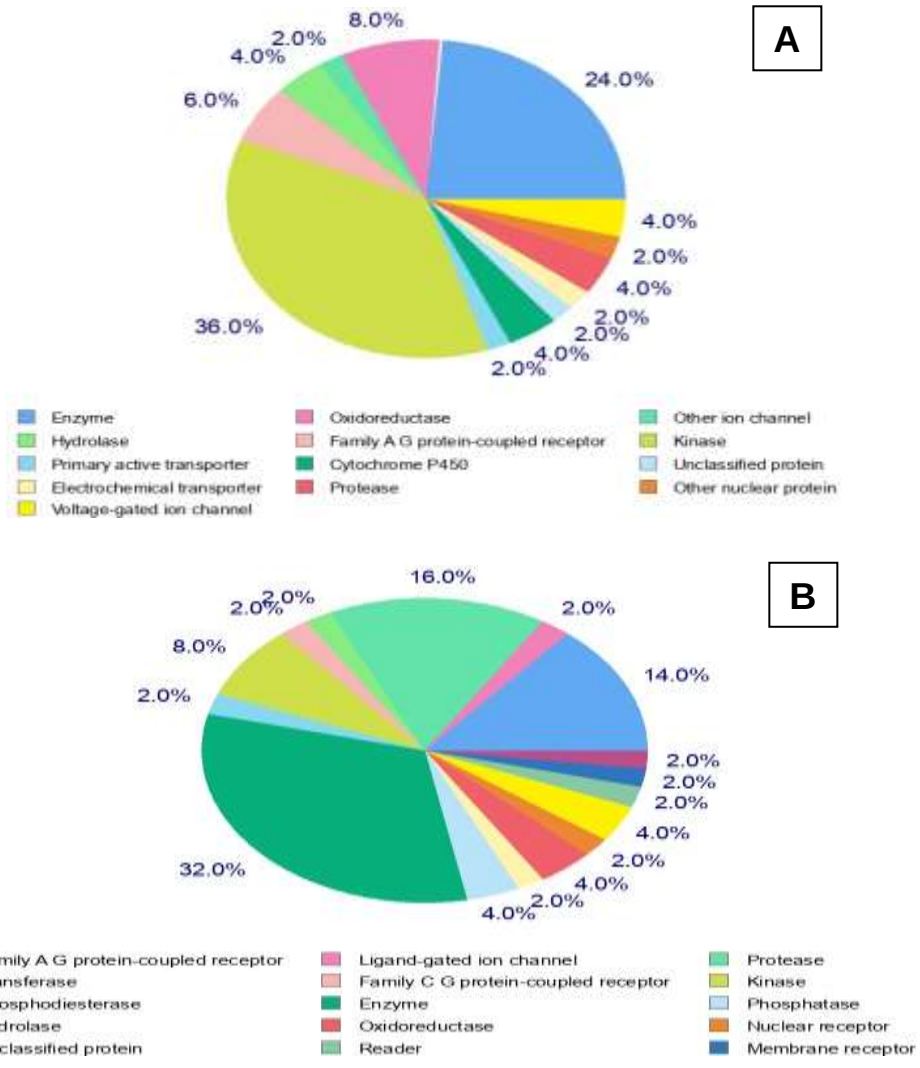

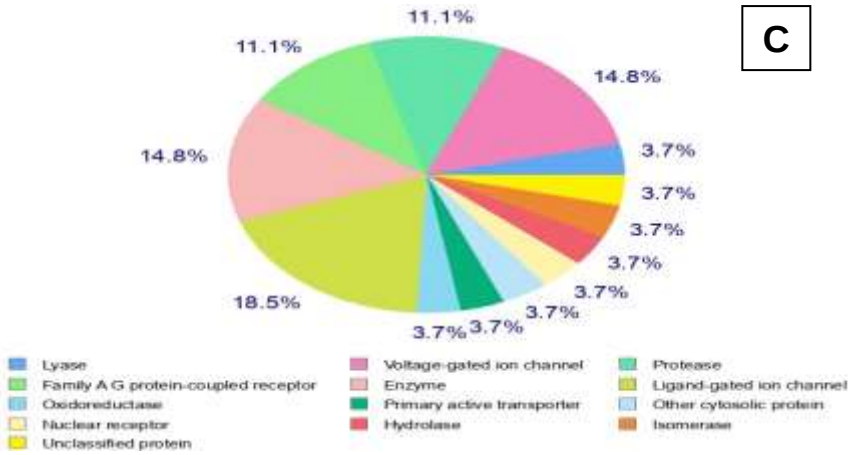

Figure 4. Predicted therapeutic targets of Compound-1 against (A) Human, (B) Mouse, and (C) Rat.

3.4.2. Compound-2

As the study is focused on determining the interacting profile of Compound-2 against therapeutic targets that have immense pharmacological perspectives, it remains crucial to exactly quantify the plausible therapeutic targets against which Compound-2 can inhibit them with micromolar concentrations, ideally. The human (*Homo sapiens*) model revealed the inhibitory perspectives of Compound-2 against the targets such as Family A G protein-coupled receptor (33.3%), Kinase (26.7%), Electrochemical transporter (13.3%), Protease (20%), and Hydrolase (6.7%) (**Figure 5**). The mouse (*Mus musculus*) model revealed the inhibitory perspectives of Compound-2 against the targets such as Family A G protein-coupled receptor (53.3%), Kinase (6.7%), Electrochemical transporter (6.7%), Unclassified protein (6.7%), Protease (20%), and Enzymes (6.7%). The rat (*Rattus norvegicus*) model revealed the inhibitory perspectives of Compound-2 against the targets such as Family A G protein-coupled receptor (33.3%), Ligand-gated ion channel (20%), Voltage-gated ion channel (6.7%), Electrochemical transporter (6.7%), Enzyme (6.7%), Kinase (6.7%), and Hydrolase (6.7%). The procured predicted results strongly supported the basis of interaction of this small molecule for possible applications against antimicrobials by revealing the possibilities of interactions with multiple targets (majorly with Family A G protein-coupled receptor).

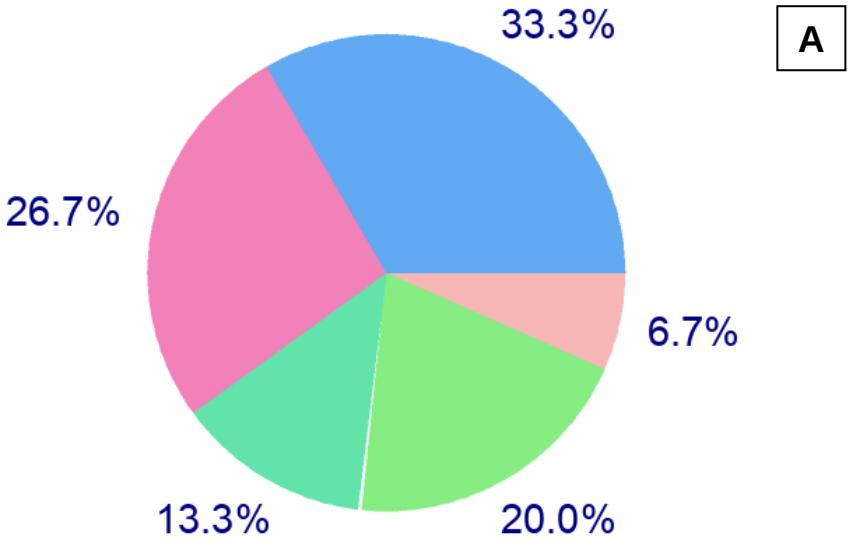

Family A G protein-coupled receptor (33.3%), **Kinase** (26.7%), **Electrochemical transporter** (13.3%), **Protease** (20%), **Hydrolase** (6.7%)

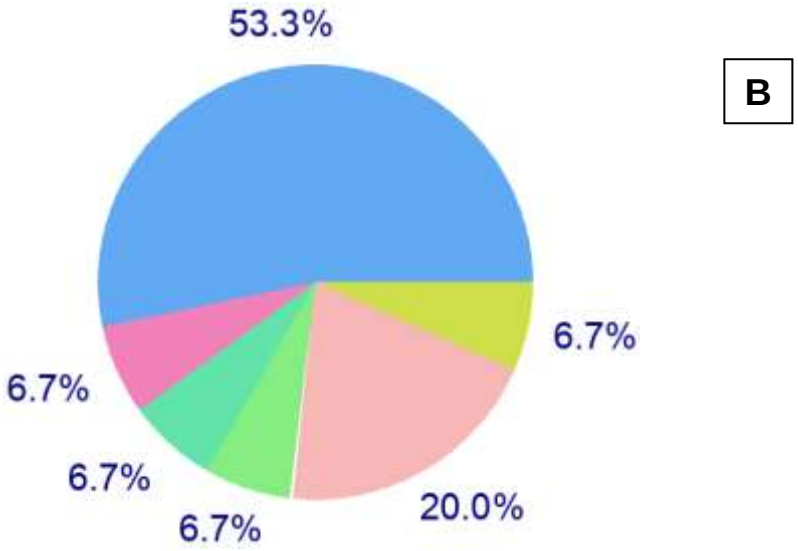

Family A G protein-coupled receptor (53.3%), **Kinase** (6.7%), **Electrochemical transporter** (6.7%), **Unclassified protein** (6.7%), **Protease** (20%), **Enzymes** (6.7%)

Family A G protein-coupled receptor (33.3%), **Ligand-gated ion channel** (20%), **Voltage-gated ion channel** (6.7%), **Electrochemical transporter** (6.7%), **Enzyme** (6.7%), **Kinase** (6.7%), **Hydrolase** (6.7%)

Figure 5. Predicted therapeutic targets of Compound-2 against (A) Human, (B) Mouse, and (C) Rat.

3.4.3. Compound-3

As the study is focused on determining the interacting profile of Compound-3 against therapeutic targets that have immense pharmacological perspectives, it remains crucial to exactly quantify the plausible therapeutic targets against which Compound-3 can inhibit them with micromolar concentrations, ideally. The human (*Homo sapiens*) model revealed the inhibitory perspectives of Compound-3 against the targets such as Family A G protein-coupled receptor (40%), secreted proteins (20%), other cytosolic protein (20%), enzymes (13.3%), and kinase (6.7%). The mouse (*Mus musculus*) model revealed the inhibitory perspectives of Compound-3 against the targets such as Family A G protein-coupled receptor (40%), kinase (6.7%), enzymes (6.7%), nuclear receptor (6.7%), transcription factor (6.7%), unclassified protein (6.7%), electrochemical transporter (6.7%), and other cytosolic protein (6.7%). The rat (*Rattus norvegicus*) model revealed the inhibitory perspectives of Compound-3 against the targets such as Family A G protein-coupled receptor (40%), enzymes (13.3%), voltage-gated ion channel (6.7%), ligand-gated ion channel (6.7%), kinase (6.7%), nuclear receptor (6.7%), and unclassified protein (6.7%) (**Figure 6**). The procured predicted results strongly supported the basis of interaction of this small molecule for possible applications against antimicrobial targets by revealing the possibilities of interactions with multiple targets (majorly with Family A G protein-coupled receptor).

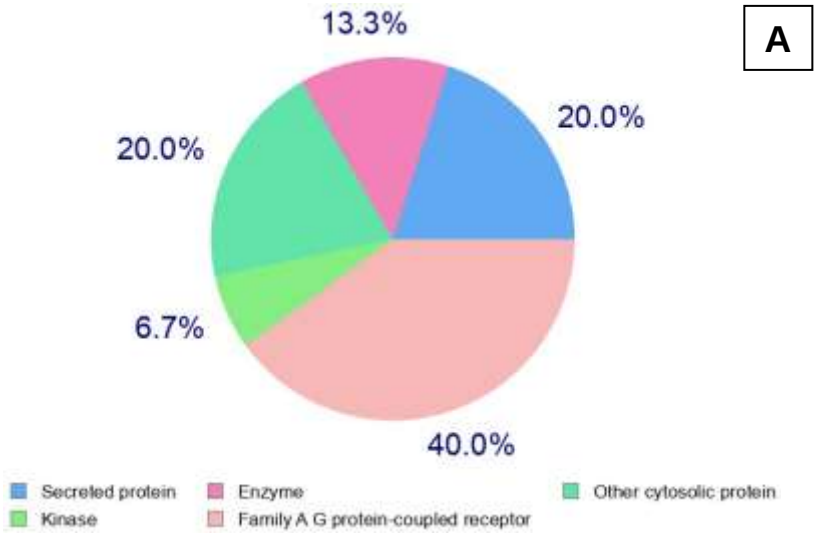

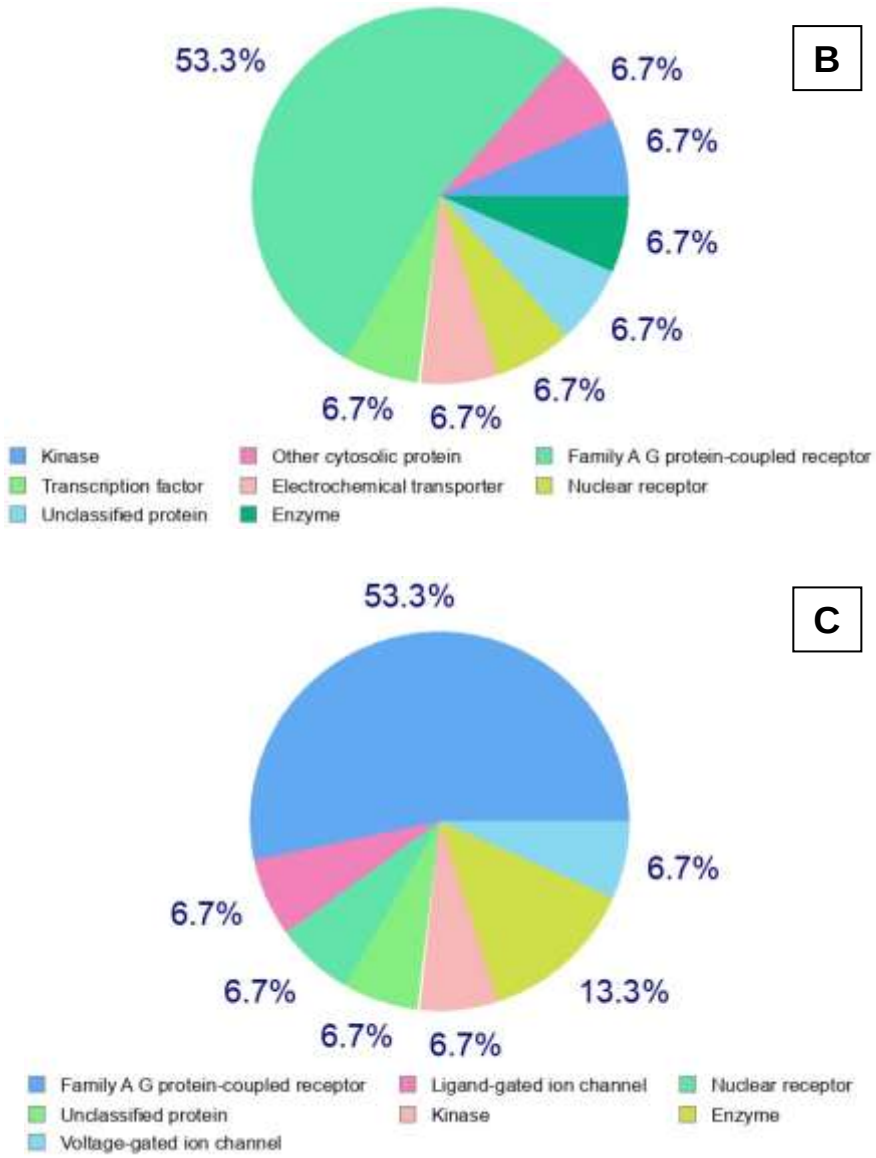

Figure 6. Predicted therapeutic targets of Compound-3 against (A) Human, (B) Mouse, and (C) Rat.

3.5. Degradation pathways for molecules

A pathway tree analysis predicts the sequential biochemical reactions that Indole might undergo, leading to its breakdown into simpler molecules. This approach combines known enzymatic reactions and metabolic pathways commonly involved in the degradation of similar compounds. The degradation of Indole is likely initiated by hydroxylation, a common metabolic transformation that introduces hydroxyl groups into the molecule. Cytochrome P450 enzymes, which are abundant in the liver, typically mediate this reaction. The initial hydroxylation could occur at the aromatic ring, resulting in the formation of a hydroxylated intermediate (**Figure 7**).

Following hydroxylation, the molecule may undergo further hydroxylation to form a catechol structure (adjacent dihydroxyl groups on the aromatic ring). This step enhances the molecule's solubility and prepares it for further metabolic processing. The catechol intermediate can undergo O-methylation, where one or both hydroxyl groups are methylated by catechol-O-methyltransferase (COMT). This step converts the dihydroxyl groups into methoxy groups, forming methoxy derivatives. The methoxy derivatives or the remaining hydroxyl groups can further undergo conjugation reactions such as glucuronidation or sulfation. These reactions enhance the solubility and facilitate the excretion of the compound from the body (**Figure 8**).

Enzymatic cleavage of the aromatic rings can occur, leading to the breakdown of the structure into smaller, more manageable fragments. This step is typically mediated by dioxygenases that cleave the aromatic ring between hydroxylated carbons, resulting in ring-opened products. The side chains of Indole can undergo beta-oxidation, a process commonly associated with fatty acid degradation. This step reduces the length of the aliphatic chains, producing acetyl-CoA and shorter carboxylic acids. The final breakdown products of Indole are typically small organic acids, alcohols, and CO_2, which are easily excreted from the body. The conjugated metabolites, such as glucuronides and sulfates, are excreted via urine or bile (**Figure 9**).

3.5.1. Compound-1

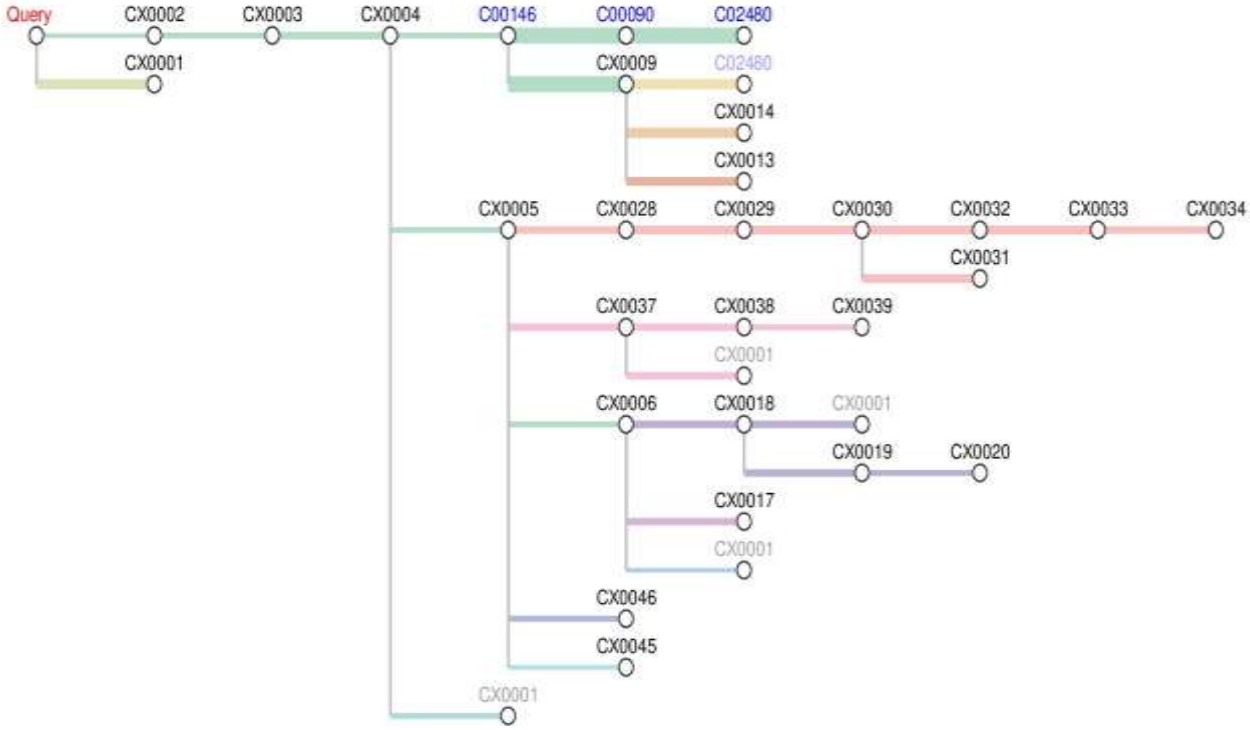

Figure 7. Predicted Pathway Tree for Compound-1.

3.5.2. Compound-2

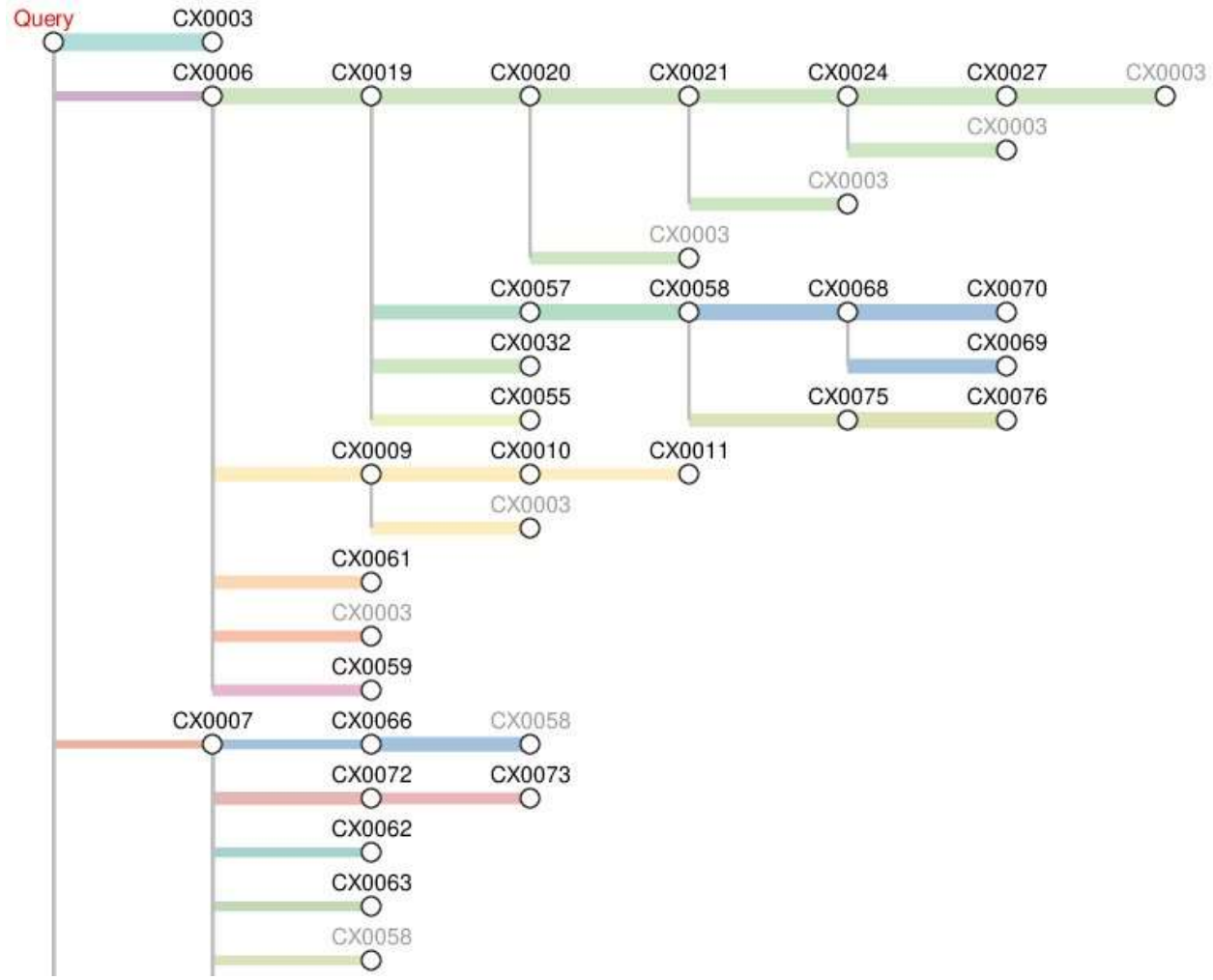

Figure 8. Predicted Pathway Tree for Compound-2.

3.5.3. Compound-3

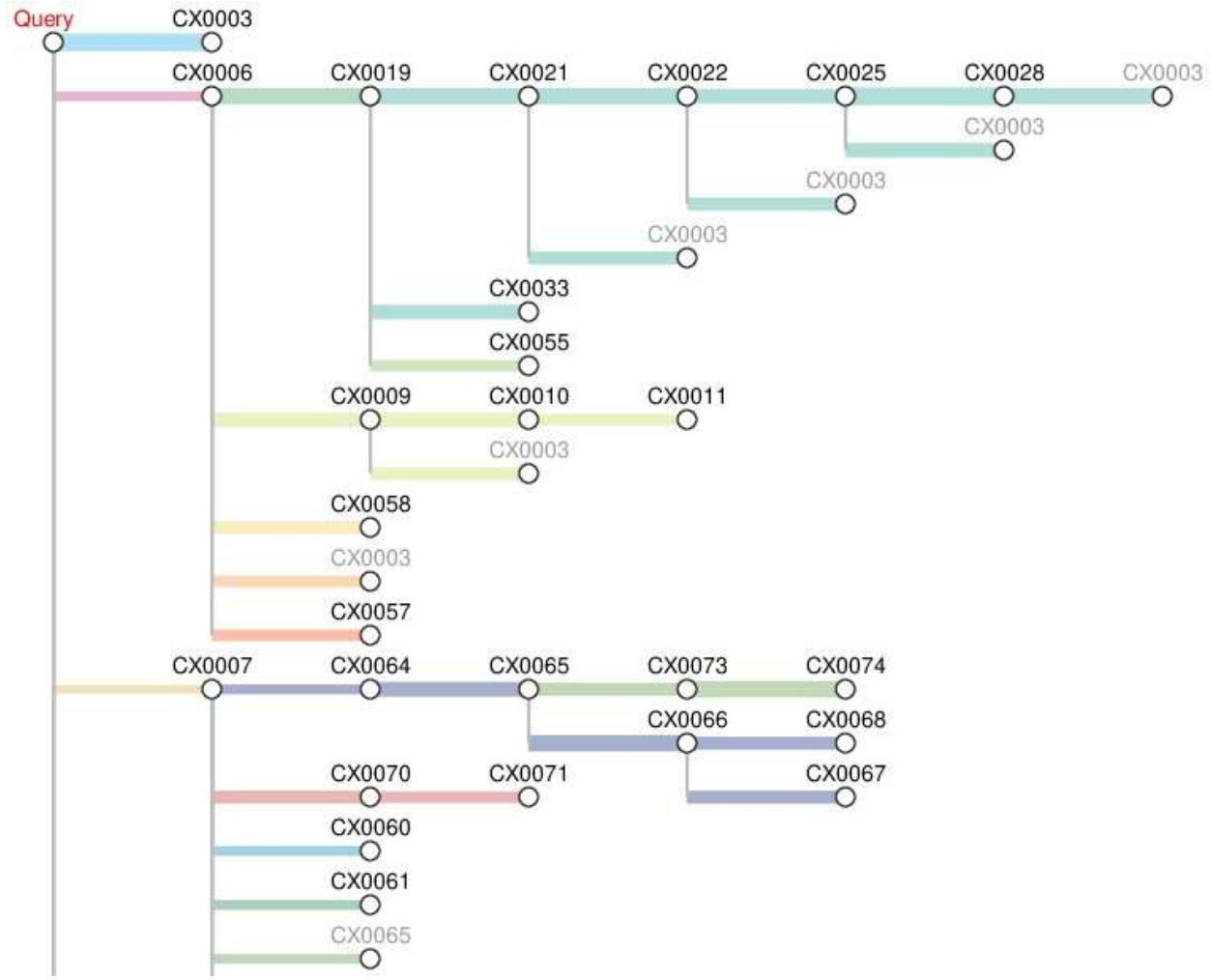

Figure 9. Predicted Pathway Tree for Compound-3.

3.9. Physical characterization of novel Indole derivatives

3.9.1. Appearance

The final compound was found to be solid, white in color, and crystalline in nature (**Table 2**).

Table 2. Characterization of novel Indole derivatives.

Characteristics	Compound-1	Compound-2	Compound-3
Appearance	White crystalline solid	Yellow amorphous solid	Yellow crystalline solid
Yield (%)	64.55	73.62	81.23
Melting point (°C)	218-219	159-161	181-182
Rf value	0.54	0.43	0.77

3.9.2. Yield

The compounds **(1-3)** were observed to be marginal (64%), moderate (73%), and 81% (significant), respectively. On consecutive purification through column chromatography, the purity of the products were ascertained, however, the quantity was less.

3.9.3. Melting point

Through digital melting point apparatus, the melting point of the compounds **(1-3)** was detected to be 218-219°C, 159-161°C, and 181-182°C. This study revealed the conversion of intermediate product into the compounds.

3.9.4. Rf value

Using the mobile phase composition of acetonitrile: ethylacetate (6:4 v/v), the Rf values of the final compound was observed to be 0.54 (for compound-1), 0.43 (for compound-2), and 0.77 (for compound-3). This study revealed the successful formation of all the novel Indole derivatives.

3.10. Spectroscopic characterization of final compound

3.10.1. FTIR Spectroscopy

The spectroscopy study supported the formation of the compound. The disappearance of (-Cl) component (655 cm^{-1}) and the appearance of NH at 3274 cm^{-1} confirmed the formation of the novel Indole derivative. The C-N component at 1701 cm^{-1} substantiates the presence of the newly added six-membered portion to the parent molecule **(Figure 10)**.

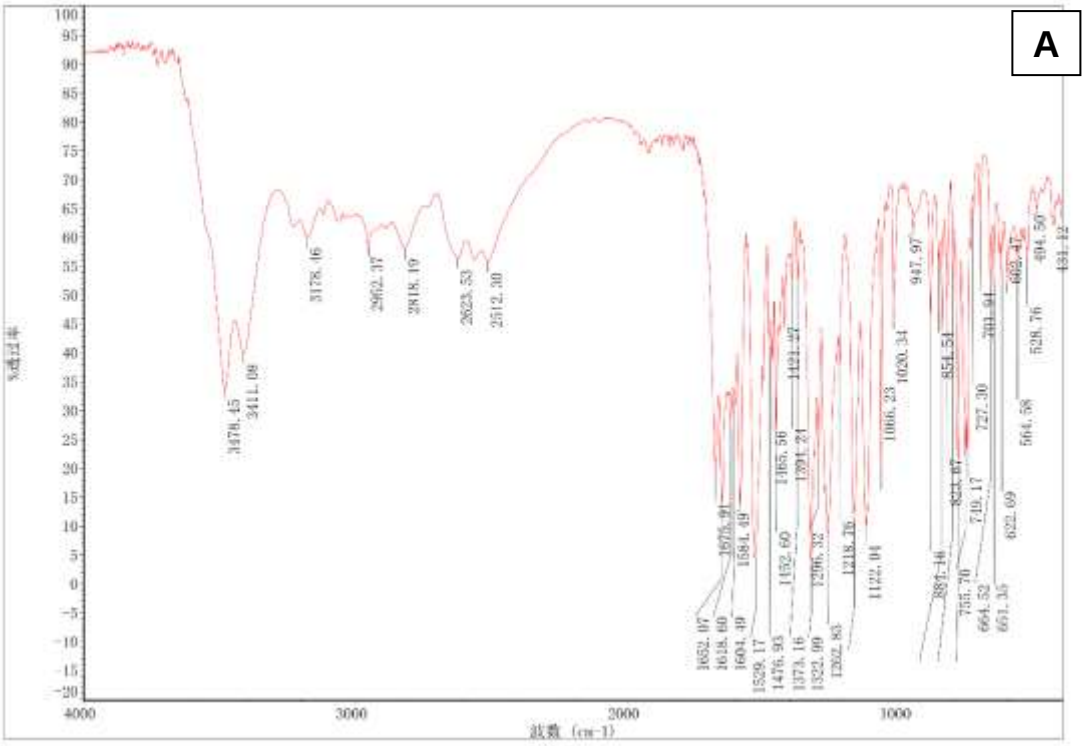
A
3478.45
3411.09
3178.16
2962.37
2818.19
2623.53
2512.30
1652.07
1618.60
1584.49
1529.17
1476.93
1373.16
1322.99
1202.83
1122.04
1066.25
1020.34
947.97
881.46
854.51
823.67
758.70
727.30
719.17
664.52
651.35
622.69
564.58
528.76
494.50
481.82
3438.66
3128.16
1772.53
1676.74
1603.99
1586.23
1532.78
1511.02
1471.20
1452.44
1418.90
1399.44
1269.00
1214.23
1179.81
1157.33
1110.57
1035.23
777.09
744.98
%透过率
波数 (cm-1)

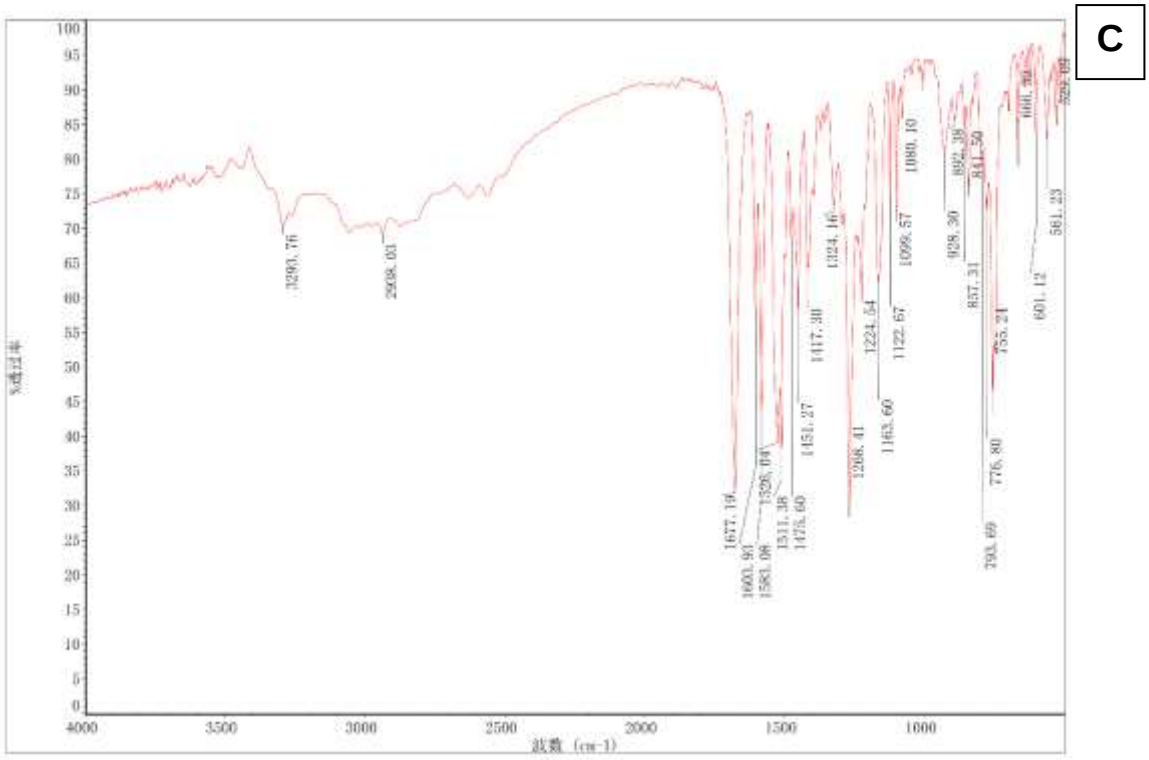

Figure 10. FTIR spectrum of novel Indole derivatives (A) Compound-1, (B) Compound-2, and (C) Compound-3.

3.10.2. ^{1}H-NMR Spectroscopy

The ^{1}H-NMR spectra represented few key aspects. The spectral range of 7.0-8.0 ppm emphasizes the presence of protons in the compound. Additionally, the –NH and –OH aspects were located at 10.4 ppm and 3.39 ppm, respectively **(Figure 11)**.

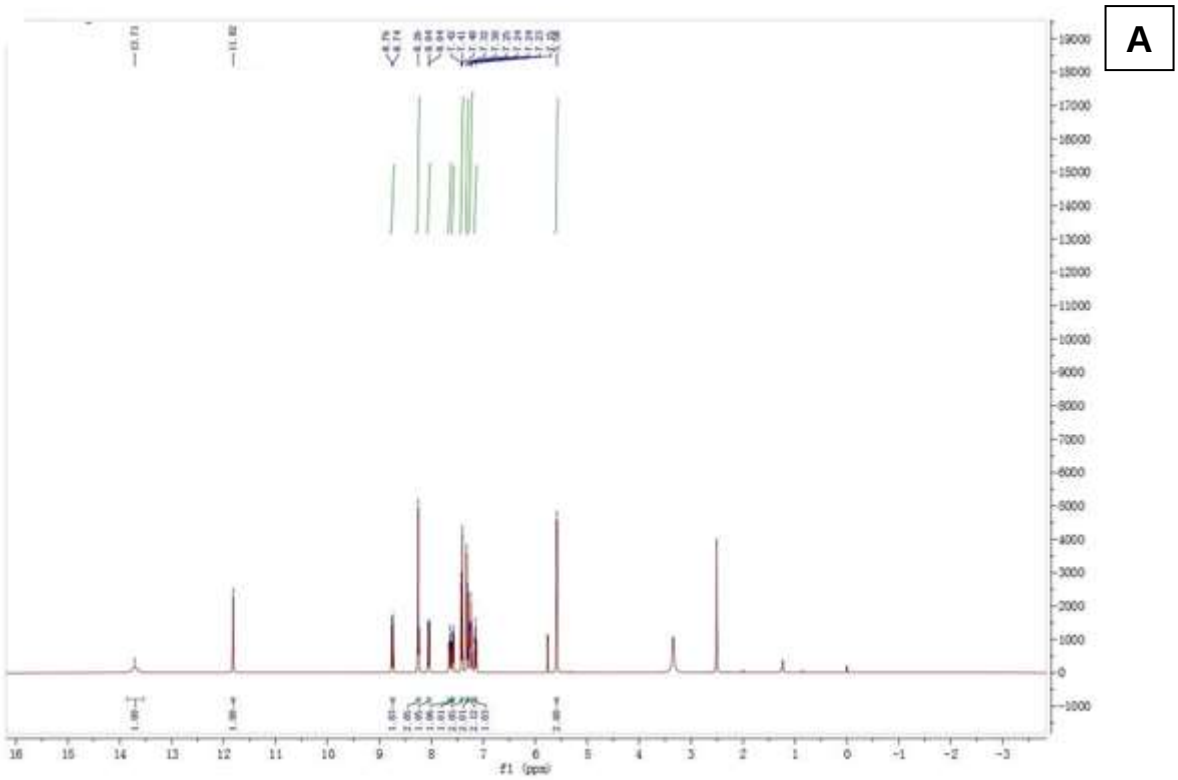
A
f1 (ppm)

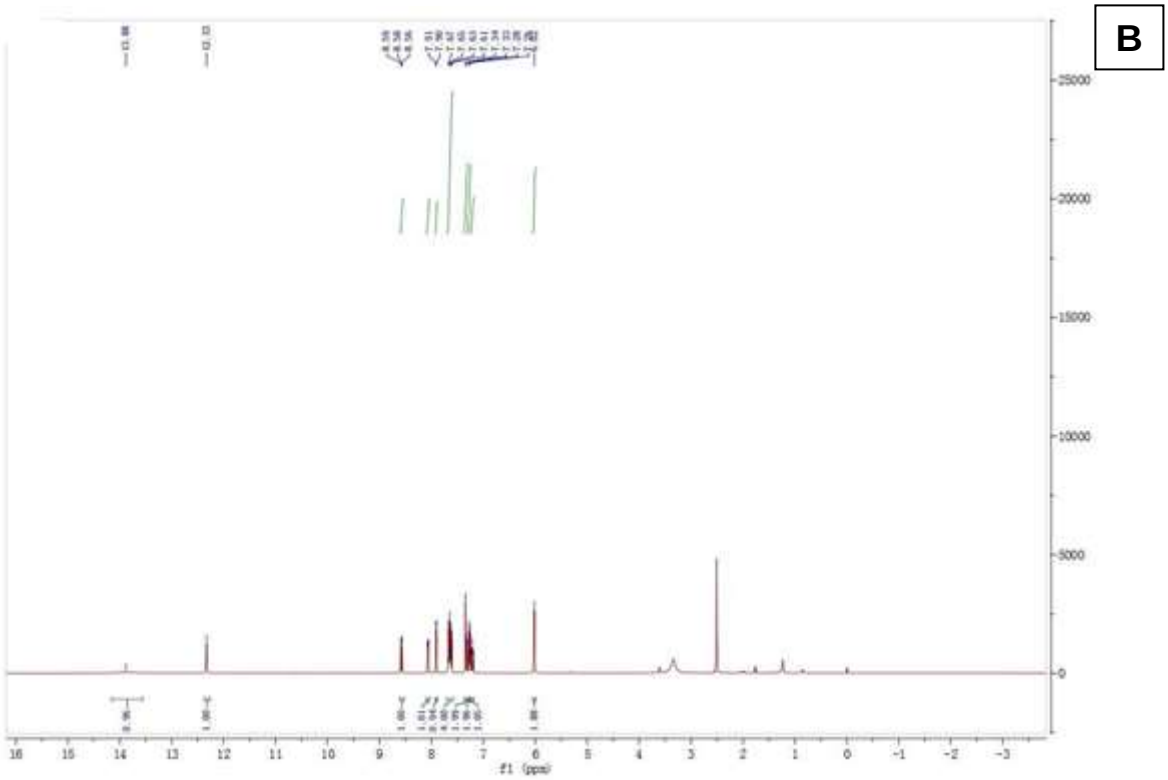
B
f1 (ppm)

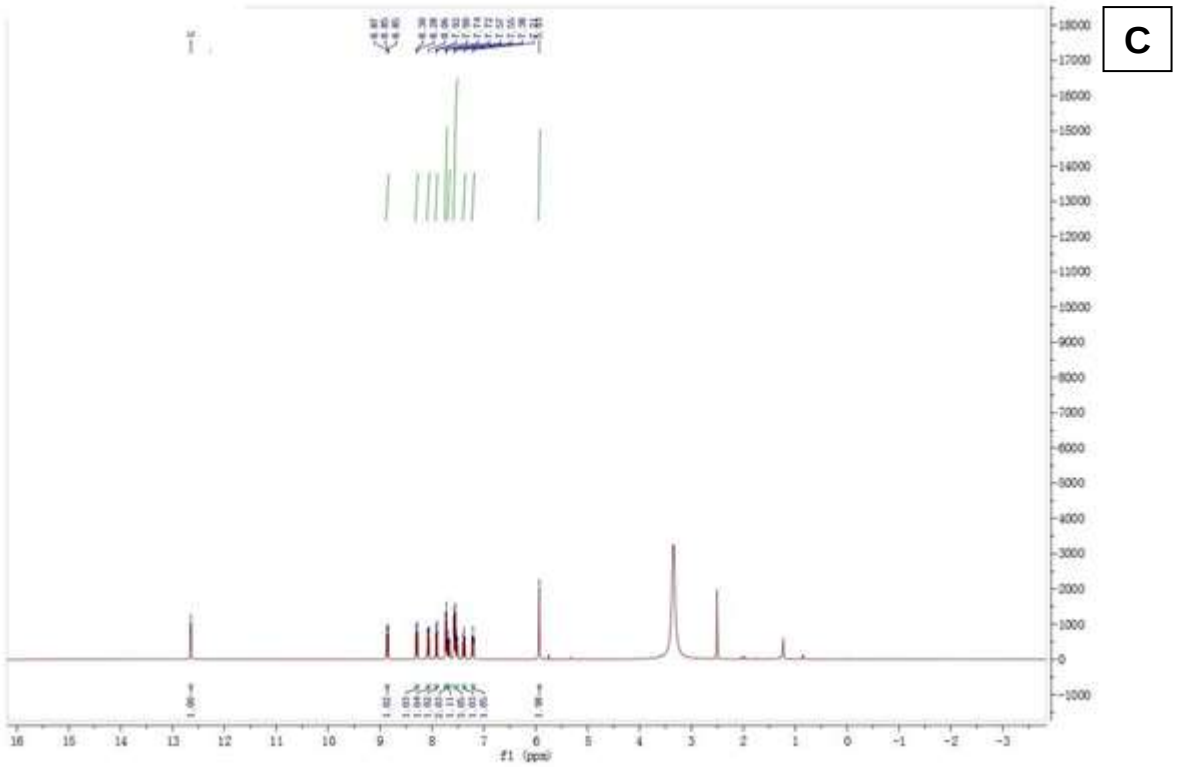

Figure 11. [1]H-NMR of novel Indole derivatives (A) Compound-1, (B) Compound-2, and (C) Compound-3.

3.10.3. [13]C-NMR Spectroscopy

The [13]C-NMR spectrum also confirmed the formation of the novel derivative and showed analogous results to that of proton NMR (**Table 3**). The spectral range of 120.0-140.0 ppm emphasizes the presence of protons in the compound. Additionally, the –NH and –OH aspects were located at 78.2 ppm and 39.6 ppm, respectively **(Figure 12)**.

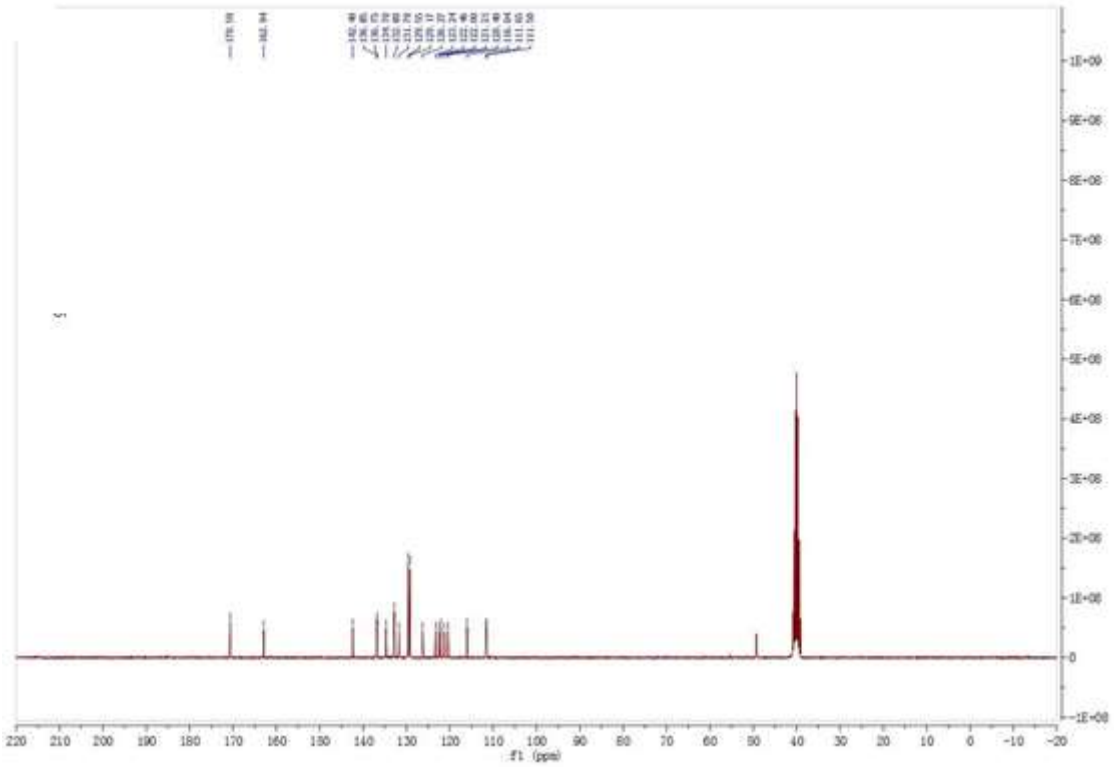
A
f1 (ppm)

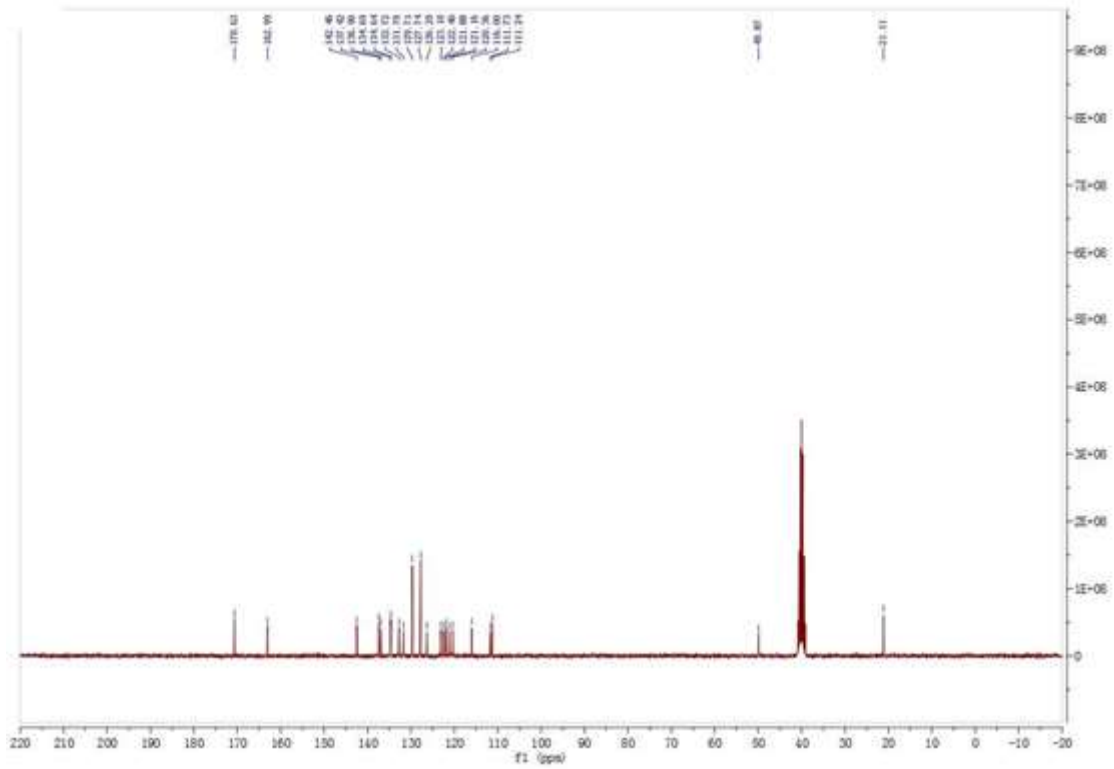
B
f1 (ppm)

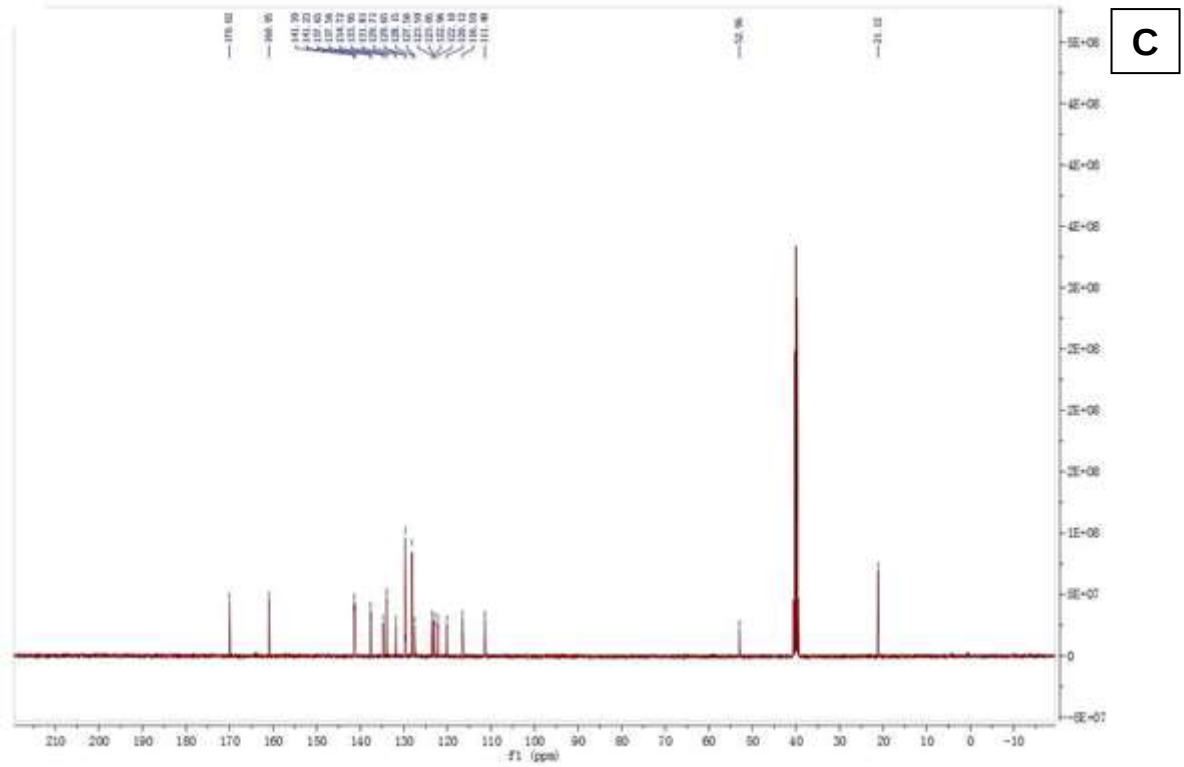

Figure 12. ^{13}C-NMR of novel Indole derivatives (A) Compound-1, (B) Compound-2, and (C) Compound-3.

3.10.4. Mass Spectroscopy

Furthermore, the mass spectra presented exactly the same molecular weight (m/z 329.04) of the fabricated molecule in the base peak. In addition to that, the fragment peaks (m/z 389.19, 373.19, 321.09, 300.19, 287.19, 256.19, 219.09, 186.19, 173.19, 149.19, 141.19, 127.09, 101.29) also appeared **(Figure 13)**.

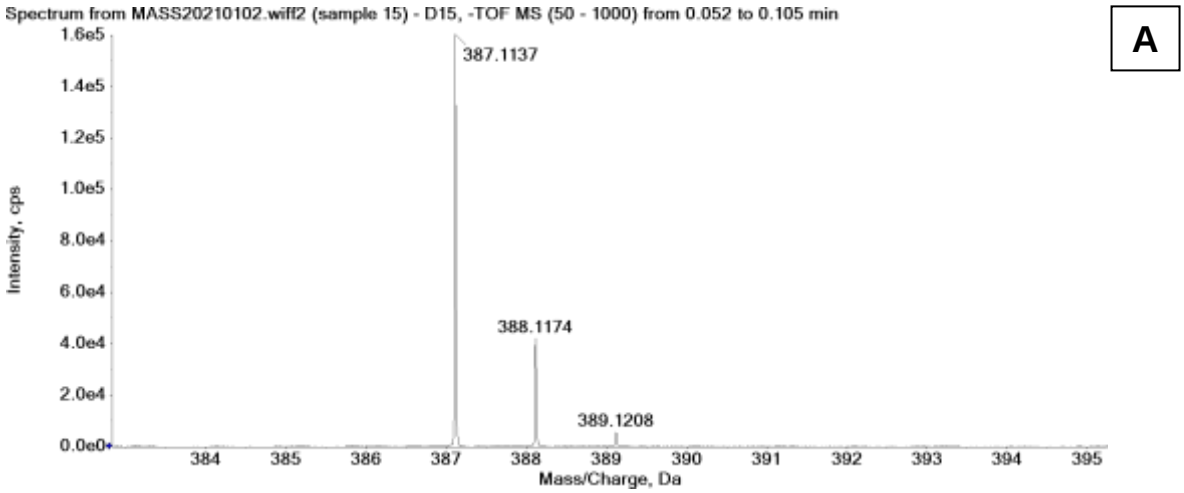

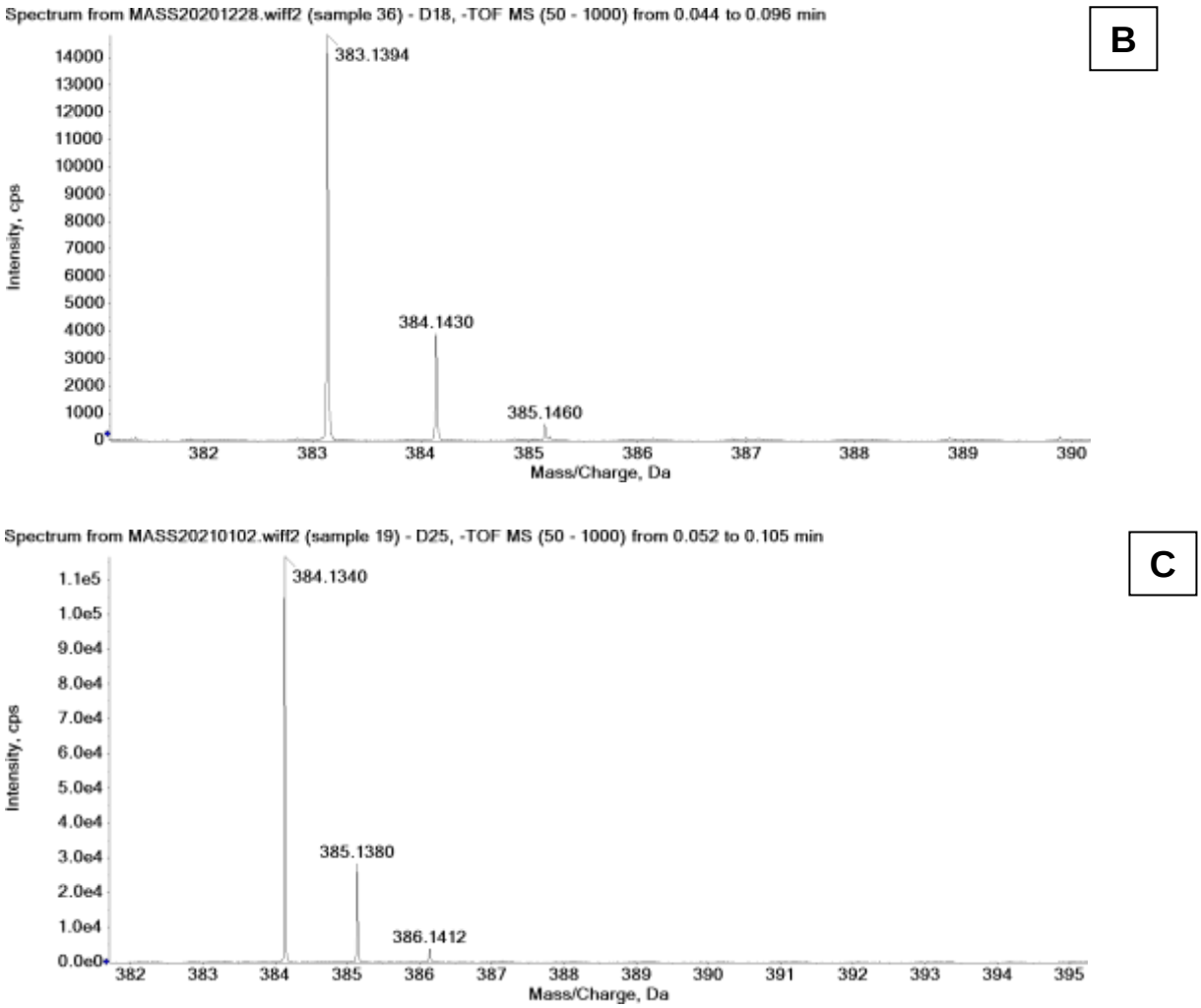

Figure 13. Mass spectra of novel Indole derivatives (A) Compound-1, (B) Compound-2, and (C) Compound-3.

Table 3. Spectral data of novel Indole derivatives.

Tools	**Characterization description**		
	Compound-1	**Compound-2**	**Compound-3**
FT-IR	3274 (-NH, stretch), 3128 (C-H, aromatic), 1737 (C=O), 1701 (C-N, stretch), 1688 (C=C, aromatic), 1620 (C=C, aromatic), 1562 (-NH, bending), 1488 ($-CH_2$), 1208 (C-O)	3280 (-NH, stretch), 3168 (C-H, aromatic), 1791 (C=O), 1713 (C-N, stretch), 1681 (C=C, aromatic), 1644 (C=C, aromatic), 1599 (-NH, bending), 1489 ($-CH_2$), 1272 (C-O)	3299 (-NH, stretch), 3183 (C-H, aromatic), 1754 (C=O), 1734 (C-N, stretch), 1698 (C=C, aromatic), 1667 (C=C, aromatic), 1576 (-NH, bending), 1495 ($-CH_2$), 1213 (C-O)
^{1}H-NMR	δ 0.99 (3H, t, *J* = 7.4 Hz), 2.65 (2H, q, *J* = 7.4 Hz), 7.10-7.32 (5H, 7.16 (dddd, *J* = 7.8,	δ 0.93-1.05 (6H, 0.99 (d, *J* = 6.7 Hz), 0.99 (d, *J* = 6.7 Hz)), 1.18-1.32 (2H, 1.25 (dd, *J* = 7.7, 7.2	δ 0.93-1.05 (6H, 0.99 (d, *J* = 6.7 Hz), 0.99 (d, *J* = 6.7 Hz)), 1.18-1.32 (2H, 1.25 (dd, *J* =

	1.3, 1.0, 0.5 Hz), 7.20 (tt, *J* = 7.7, 1.3 Hz), 7.26 (tdd, *J* = 7.7, 1.6, 0.5 Hz))	Hz), 1.25 (dd, *J* = 7.7, 7.2 Hz)), 1.52 (1H, tsept, *J* = 7.2, 6.6 Hz), 1.70 (1H, dtt, *J* = 14.1, 8.9, 6.7 Hz), 1.85-2.31 (11H, 1.93 (dtt, *J* = 14.1, 6.7, 2.3 Hz), 2.08 (ddd, *J* = 14.6, 6.7, 2.3 Hz), 2.08 (ddd, *J* = 14.5, 6.7, 2.3 Hz), 2.23 (ddd, *J* = 14.6, 8.9, 6.7 Hz), 2.23 (ddd, *J* = 14.5, 8.9, 6.7 Hz), 2.25 (s)), 2.80 (1H, t, *J* = 7.7 Hz), 3.75 (3H, s), 6.29 (2H, ddd, *J* = 8.2, 1.1, 0.5 Hz), 6.67 (2H, ddd, *J* = 8.7, 2.7, 0.5 Hz), 7.04-7.17 (4H, 7.10 (ddd, *J* = 8.7, 1.7, 0.5 Hz), 7.11 (ddd, *J* = 8.2, 1.1, 0.5 Hz))	7.7, 7.2 Hz), 1.25 (dd, *J* = 7.7, 7.2 Hz)), 1.52 (1H, tsept, *J* = 7.2, 6.6 Hz), 1.70 (1H, dtt, *J* = 14.1, 8.9, 6.7 Hz), 1.85-2.31 (14H, 1.93 (dtt, *J* = 14.1, 6.7, 2.3 Hz), 2.08 (ddd, *J* = 14.6, 6.7, 2.3 Hz), 2.08 (ddd, *J* = 14.5, 6.7, 2.3 Hz), 2.23 (ddd, *J* = 14.6, 8.9, 6.7 Hz), 2.23 (ddd, *J* = 14.5, 8.9, 6.7 Hz), 2.21 (s), 2.25 (s)), 2.80 (1H, t, *J* = 7.7 Hz), 6.21-6.35 (4H, 6.27 (ddd, *J* = 8.2, 1.4, 0.5 Hz), 6.29 (ddd, *J* = 8.2, 1.1, 0.5 Hz)), 7.06 (2H, ddd, *J* = 8.2, 1.3, 0.5 Hz), 7.21 (2H, ddd, *J* = 8.2, 1.1, 0.5 Hz)
^{13}C-NMR	δ 11.3 (1C, s), 15.8 (1C, s), 20.3-20.4 (2C, 20.4 (s), 20.4 (s)), 21.3 (1C, s), 26.3-26.4 (2C, 26.4 (s), 26.4 (s)), 29.1 (1C, s), 35.6 (1C, s), 40.6 (1C, s), 41.8 (2C, s), 59.6 (1C, s), 117.9 (2C, s), 119.3 (1C, s), 119.9 (1C, s), 127.1 (1C, s), 129.0 (1C, s), 129.6 (2C, s), 139.4 (1C, s), 141.5 (1C, s), 142.0 (1C, s), 144.9 (1C, s)	δ 15.8 (1C, s), 22.5-22.6 (2C, 22.6 (s), 22.6 (s)), 24.4 (1C, s), 26.3-26.4 (2C, 26.4 (s), 26.4 (s)), 35.1 (1C, s), 40.6 (1C, s), 41.8 (2C, s), 56.0 (1C, s), 60.1 (1C, s), 114.5 (2C, s), 117.9 (2C, s), 120.5 (2C, s), 127.4 (2C, s), 141.9-142.1 (2C, 142.0 (s), 142.0 (s)), 144.9 (1C, s), 159.8 (1C, s)	δ 15.8 (1C, s), 21.3 (1C, s), 22.5-22.6 (2C, 22.6 (s), 22.6 (s)), 24.4 (1C, s), 26.3-26.4 (2C, 26.4 (s), 26.4 (s)), 35.1 (1C, s), 40.6 (1C, s), 41.8 (2C, s), 60.1 (1C, s), 117.9-118.0 (4C, 117.9 (s), 117.9 (s)), 127.4 (2C, s), 129.6 (2C, s), 141.5 (1C, s), 141.9-142.1 (2C, 142.0 (s), 142.0 (s)), 144.9 (1C, s)
Mass	m/z 329; Fragments: 389.19, 373.19, 321.09, 300.19, 287.19	m/z 350; Fragments: 256.19, 186.19, 127.09, 101.29	m/z 366; Fragments: 219.09, 173.19, 149.19, 141.19
CHN Analysis	Theoretical: C, 64.39; H, 5.20; Cl, 7.31; O, 16.49; S, 6.61 Practical:	Theoretical: C, 61.14; H, 5.39; Cl, 9.02; O, 16.29; S, 8.16 Practical:	Theoretical: C, 64.93; H, 6.23; O, 20.59; S, 8.25 Practical:

C, 61.14; H, 4.99	C, 59.12; H, 5.03	C, 60.54; H, 5.93

3.11. Anti-microbial study

The results of antibacterial screening of Compound-1, Compound-2, Compound-3, and Standard compound are shown in **Table 4**. Compound-3 showed low anti-bacterial activity whereas Compound-1 expressed moderate anti-bacterial activity with average MIC value against *E. coli* and *B. subtilis* (**Figure 14**). In contrast to them, Compound-2 presented highest anti-bacterial activity, however, the activity was less pronounced than the standard drug Clindamycin.

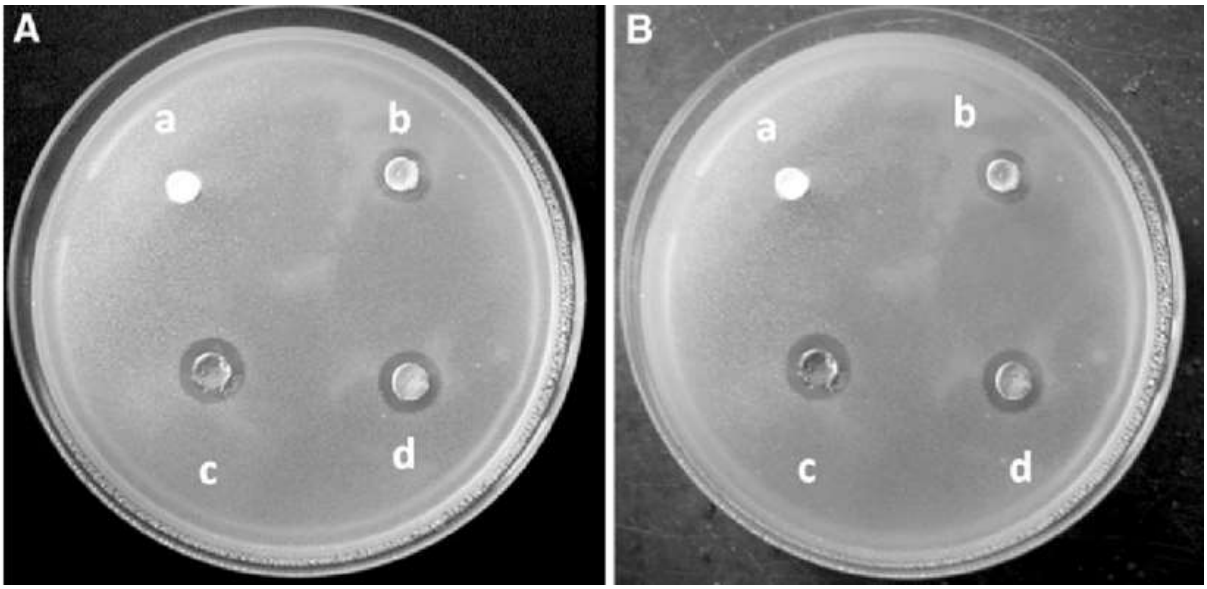

Figure 14. Pictures of microbial plates (A) *E. coli* (B) *B. subtilis*. (a) Compound-1 (b) Compound-2 (c) Compound-3 (d) Standard compound (Clindamycin).

Table 4. Anti-microbial activity of Compound-1, Compound-2, Compound-3, and Standard compound.

Components	***E. coli***	***B. subtilis***
Clindamycin [#]	29.9 ± 1.57 (6.25)	28.1 ± 1.15 (6.25)
Compound-1	22.4 ± 1.37*** (25)	20.2 ± 1.47*** (25)
Compound-2	24.1 ± 1.72*** (25)	23.6 ± 1.69*** (25)
Compound-3	20.7 ± 1.44*** (25)	21.9 ± 1.31*** (25)

All values represent mean ± SEM of n = 3; ***p<0.001. Zone of inhibition of test compounds against microbes are measured in mm. Values inside the bracket represents the minimum inhibitory concentration (MIC). [#] Standard reference for anti-bacterial activity

4. CONCLUSION

The study adopts a rational approach that integrates principles of synthetic organic chemistry, structural modification, and antimicrobial evaluation to identify potential candidates with enhanced biological activity. The comprehensive investigation includes the

design, synthesis, characterization, and biological screening of indole derivatives, with an emphasis on elucidating the structure-activity relationship (SAR). The synthetic pathway for indole derivatives was meticulously designed to introduce specific substituents at key positions on the indole nucleus to enhance its antimicrobial potential. The choice of substituents was guided by literature evidence and computational predictions, ensuring the rational design of molecules with the highest likelihood of biological activity. The synthetic strategy employed involved classical and modern synthetic techniques, including condensation, cyclization, and nucleophilic substitution reactions. The overall yield, purity, and reproducibility of each step were optimized to ensure an efficient and scalable synthesis process. Spectroscopic characterization of the synthesized compounds was conducted using state-of-the-art analytical techniques, such as Fourier Transform Infrared (FTIR) Spectroscopy, Nuclear Magnetic Resonance (NMR) Spectroscopy (^{1}H and ^{13}C NMR), Mass Spectrometry (MS), and Ultraviolet-Visible (UV-Vis) Spectroscopy. The characterization data confirmed the successful synthesis of target indole derivatives and provided detailed insight into their structural features. The FTIR spectra verified the presence of functional groups like –OH, –NH, and –C=O, while the NMR spectra offered precise information about the position and nature of protons and carbons in the molecules. Mass spectrometric analysis confirmed the molecular weight and fragmentation pattern of the derivatives, further validating the structural integrity of the synthesized compounds.

The antimicrobial potential of the synthesized indole derivatives was evaluated against a broad spectrum of pathogenic microorganisms, including Gram-positive bacteria (*Bacillus subtilis*) and Gram-negative bacteria (*Escherichia coli*). The results revealed that several derivatives exhibited significant antimicrobial activity, with certain compounds showing higher efficacy than standard reference drugs. The Minimum Inhibitory Concentration (MIC) values highlighted the potency of specific derivatives, suggesting their potential for further development as novel antimicrobial agents. The results were systematically analyzed to establish a structure-activity relationship (SAR), which revealed that electron-donating groups at specific positions on the indole nucleus significantly influence antimicrobial activity. One of the key findings of this study is the identification of lead compounds that demonstrated superior antimicrobial efficacy compared to standard reference drugs. Certain derivatives exhibited dual-action antibacterial and antifungal properties, which is a critical advantage in addressing the growing challenge of antimicrobial resistance (AMR). The SAR analysis indicated that the presence of electron-donating substituents, at specific positions of the indole scaffold enhanced bacterial inhibition. This information provides a valuable basis for the future design of novel indole-based therapeutics with multi-target antimicrobial activity.

The findings of this study have significant implications for pharmaceutical research and development. The indole scaffold has proven to be a privileged structure for the development of bioactive molecules, and the successful synthesis of novel derivatives with enhanced antimicrobial properties underscores the potential of indole chemistry in drug discovery. The derivatives synthesized in this study can serve as lead molecules for future antimicrobial drug development programs. Moreover, the established synthetic methodology

and structure-activity insights could be further applied to design other biologically active indole derivatives with potential applications in combating antimicrobial resistance (AMR), a global health threat. This research also sheds light on the potential use of indole derivatives as alternatives to conventional antibiotics. In an era where resistance to existing antibiotics is on the rise, the development of novel antimicrobial agents with unique mechanisms of action is of paramount importance. The ability of the synthesized derivatives to target both Gram-positive and Gram-negative bacteria, as well as fungi, highlights their broad-spectrum potential. As a result, these derivatives could be further explored as candidates for the development of next-generation antimicrobials to address the pressing issue of drug-resistant infections.

CONFLICT OF INTEREST

No Conflict of Interest is declared.

ACKNOWLEDGEMENT

No person is acknowledged.

FUNDING INFORMATION

No agency provided any funding.

5. REFERENCES

Abdel-Mohsen AM, Abdel-Rahman RM, Hrdina R, Burgert L, Aly AS, Hebeish A. Antimicrobial activity of hyaluronan-based fiber with silver nanoparticles. Carbohydr Polym. 2013;92(2):1177–87.

Aboul-Fadl T, Bin-Jubair FA. Synthesis, antimicrobial and antitumor evaluation of novel indole derivatives. Eur J Med Chem. 2010;45(12):6527–33.

Adams DJ, Butler MS. Antimicrobial resistance: the need for novel antibiotics. Curr Opin Microbiol. 2021;63:62–9.

Ahmad I, Beg AZ. Antimicrobial and phytochemical studies on 45 Indian medicinal plants against multi-drug resistant pathogens. J Ethnopharmacol. 2001;74(2):113–23.

Ahmed N, Anwar F, Zia-ur-Rehman M, Shahid M. Synthesis, antimicrobial and antioxidant activities of novel indole derivatives. Eur J Med Chem. 2012;54:724–30.

Ahsan F, Rivas IP, Khan MA, Torres Suárez AI. Role of physicochemical properties of particulate carriers on macrophage uptake. J Control Release. 2002;79(1–3):29–40.

Akinboye ES, Bakare O. Biological activities of indole derivatives: A review. Stud Nat Prod Chem. 2011;36:485–558.

Alagarsamy V, Raja S, Ramanathan M. Synthesis and anti-inflammatory activity of indole derivatives. Bioorg Med Chem Lett. 2006;16(5):998–1001.

Ali I, Haque A, Wani WA, Saleem K. Platinum compounds as anticancer agents. Anticancer Agents Med Chem. 2013;13(2):296–306.

Alves MJ, Ferreira IC, Dias J, Teixeira V, Martins A, Pintado M. Antimicrobial activity of mushroom extracts and compounds. Food Chem. 2012;130(3):519–26.

Anbazhagan S, Chidambaram R, Singaravadivel S. Antimicrobial activity of novel indole derivatives against clinical isolates. Indian J Chem. 2020;59(8):1043–52.

Bansal Y, Silakari O. The therapeutic potential of benzimidazole derivatives: a review. Bioorg Med Chem. 2012;20(21):6208–46.

Bhandari R, Khurana RK, Kaur R, Kaur R. A comprehensive review on the pharmacological potential of indole derivatives. J Chem Pharm Res. 2015;7(10):779–92.

Bhardwaj VK, Singh R, Sharma J, Das P, Purohit R. Inhibitory potential of withaferin A against SARS-CoV-2 main protease. J Biomol Struct Dyn. 2021;39(16):6257–68.

Caruso F, Hyeon T, Rotello VM. Nanomedicine: Current trends and future prospects. Nanotechnology. 2021;15:88–93.

Cechinel Filho V, Yunes RA. Strategies for bioactive natural product isolation. Plant Bioact Drug Discov. 2012;1–19.

Chen Z, Cheng L, He J, Jiang X. Synthesis and antimicrobial evaluation of novel indole derivatives. Eur J Med Chem. 2016;122:95–104.

Chopra I, Hodgson J, Metcalf B, Poste G. Challenges in antimicrobial drug discovery. Antimicrob Agents Chemother. 1997;41(3):497–503.

Cragg GM, Newman DJ. Natural products as sources of new drugs. Biochim Biophys Acta. 2013;1830(6):3670–95.

Das P, Tiwari A, Srivastava A, Mishra S. Design, synthesis, and antimicrobial activity of novel indole derivatives. Chem Biol Interact. 2020;317:108968.

De Souza PC, Santos JB, Nascimento RA, Batista AM. Novel indole-based compounds with potent antimicrobial activity. Bioorg Med Chem. 2022;34:115985.

Denny WA. Antimicrobial quinolones: Recent developments. Curr Opin Chem Biol. 2002;6(5):547–56.

Ebrahimi SN, Hamedeyazdan S, Smiesko M, Hamburger M. Antimicrobial activity of synthetic indole derivatives. Phytochem Rev. 2013;12(4):945–72.

Ecker GF, Chiba P. Structure-activity relationships of efflux pump inhibitors. J Med Chem. 2009;52(17):5342–57.

Elgemeie GH, El-Ashry EH, Shaaban MR. Synthesis of new indole-based antimicrobial agents. J Heterocycl Chem. 2018;55(7):1551–60.

El-Kashef H, Abdel-Aziz H. Antibacterial activity of indole derivatives against Gram-positive and Gram-negative bacteria. Acta Pharm. 2020;70(3):315–25.

Evans JT, Fiser R, Kim KH, Lee JM, Weissman JS. Drug resistance mechanisms in pathogens. Nat Rev Drug Discov. 2018;17(7):505–24.

Fiers W, de Oliveira GP, Nascimento C, Taveira S. Indole-3-carbinol as an antimicrobial agent. Int J Antimicrob Agents. 2019;53(2):135–43.

Gholivand K, Omidi S, Hashemi M. Design and synthesis of indole derivatives as antimicrobial agents. Med Chem Res. 2017;26(9):2071–9.

Goodwin AC, Jenkins M, Chittick T. Biological activity of indole-based molecules. Curr Drug Targets. 2019;20(2):128–45.

Gupta A, Mishra R, Jaiswal DK, Rajput S. Synthesis and antimicrobial activity of novel 2,3-disubstituted indole derivatives. Eur J Med Chem. 2017;126:955–65.

Hansch C, Leo A, Taft RW. A survey of Hammett substituent constants and resonance and field parameters. Chem Rev. 1991;91(2):165–95.

Hassanpour S, Jahanshahi M, Taherzadeh M. Recent developments in antimicrobial indole derivatives. Mol Divers. 2022;26(3):541–59.

Hebeish A, Abdel-Mohsen AM, Aly AS. Antimicrobial properties of modified polysaccharides. Carbohydr Polym. 2013;92(2):1177–87.

Hussain A, Yadav A, Soni V. Recent developments in the synthesis and biological evaluation of novel indole derivatives. Bioorg Med Chem. 2020;28(4):115095.

Jamkhande PG, Ghante MH, Jadhav SL, Bamer AH. Indole derivatives with diverse therapeutic applications. J Mol Struct. 2020;1203:127353.

Javed H, Khan MM, Ahmad A, Vaibhav K. Indole-based therapeutic scaffolds: A review. Chem Biol Interact. 2020;317:108968.

Joshi M, Rana AC, Soni P, Rana S. Novel indole derivatives as antimicrobial agents: A review. Asian J Chem. 2017;29(1):1–10.

Kesharwani T, Prajapati B, Pandey R. Structure-activity relationship of indole derivatives as antimicrobial agents. J Chem Pharm Res. 2016;8(8):1–12.

Kumar D, Sharma A, Bansal S. Development of potent antimicrobial indole derivatives: A review. Int J Pharm Pharm Sci. 2018;10(2):54–62.

Lamba V, Negi A, Sharma N. Structure-based design of indole derivatives as antimicrobial agents. J Chem Pharm Res. 2020;12(7):97–115.

Li X, Huang Y, Yao L. Indole-based small molecules as potential antimicrobial agents. Bioorg Chem. 2019;88:102979.

Mishra S, Kumar M, Tiwari S. Rational synthesis and characterization of indole derivatives. J Heterocycl Chem. 2021;58(2):243–58.

Mohan R, Murthy R, Balasubramanian S. Indole derivatives as potential antimicrobial agents: A review. Mini Rev Med Chem. 2019;19(10):821–45.

Monge A, Palop JA, Matos MJ. Recent advances in the synthesis of antimicrobial indole derivatives. Curr Top Med Chem. 2021;21(5):385–406.

Nagaraja B, Kumar TR, Chandan RS. Synthesis and antimicrobial evaluation of substituted indole derivatives. Bioorg Med Chem Lett. 2014;24(16):3759–64.

Naim MJ, Alam O, Nawaz F. Indole derivatives as promising antimicrobial agents. Bioorg Med Chem. 2020;28(8):115518.

Nakanishi K, Solomon PH. Infrared Absorption Spectroscopy: Practical. San Diego: Academic Press; 1977. p. 52–65.

Naushad M, Ahamad T, Sharma G. Antimicrobial activity of hybrid indole derivatives. J Photochem Photobiol B. 2018;183:258–67.

Negi A, Bhatt P, Sharma P, Singh D. Synthesis and antimicrobial evaluation of 2,3-substituted indole derivatives. J Chem Pharm Res. 2019;11(3):20–8.

Newman DJ, Cragg GM. Natural product-based drug discovery. Biochim Biophys Acta. 2016;1830(6):3670–95.

Nikalje AP, Nikalje R. Antimicrobial activity of novel 2-aryl substituted indole derivatives. Int J Pharm Res. 2019;11(1):123–9.

Padmanabhan J, Parthiban C, Mohan A. Advances in indole-based drug discovery: Current status and future directions. Eur J Med Chem. 2020;207:112741.

Palumbo M, Sissi C, Pratesi G. Novel anticancer agents targeting topoisomerases. Curr Med Chem. 2002;9(8):781–9.

Patel SR, Jain B, Kumar S. Structural insights into the antimicrobial activity of indole derivatives. Indian J Chem. 2020;59(3):283–93.

Patel HA, Dalwadi SJ, Bhadania VP. Rational drug design and synthesis of new indole derivatives with antibacterial activity. Asian J Chem. 2017;29(7):1563–9.

Phan N, Huynh L, Nguyen T, Vu T. Antibacterial effects of indole-based natural products. J Nat Prod. 2018;81(9):2153–62.

Pradeep H, Prasanth D, Prasanna B, Ramesh K. Synthesis, characterization, and antibacterial evaluation of indole derivatives. J Pharm Res. 2020;14(2):210–20.

Pratibha A, Kumar N, Sharma S. Recent developments in indole-based antimicrobial agents. Curr Top Med Chem. 2021;21(6):438–54.

Rani A, Srivastava AK, Gupta S, Tandon V. Synthesis, characterization, and evaluation of indole-based hybrids as antimicrobial agents. J Heterocycl Chem. 2022;59(3):652–63.

Rana S, Kumar R, Aggarwal N. Biological activities of synthetic indole derivatives: A review. Mini Rev Med Chem. 2018;18(7):557–80.

Rao PS, Naik KS, Kumar NS. Synthesis of indole-based compounds and their antimicrobial activity. Chem Biol Drug Des. 2017;89(5):751–63.

Rathod KS, Mehta A, Sharma P. Indole derivatives as promising scaffolds in antimicrobial drug development. Eur J Med Chem. 2019;175:32–45.

Rawal RK, Muddukrishna B, Pathak R. Synthesis of novel antimicrobial agents using an indole-based scaffold. Int J ChemTech Res. 2020;12(2):98–108.

Reddy CS, Kumar R, Sharma S. Antimicrobial potential of indole derivatives against resistant pathogens. Indian J Chem. 2018;57(8):1061–72.

Ren Z, Wang Y, Liu X, Zhang J. New indole derivatives as potent antibacterial agents. Bioorg Chem. 2021;108:104681.

Rojas-Silva P, Dey M, González-Montiel J. Phytochemical profiling and antibacterial activity of selected medicinal plants. J Ethnopharmacol. 2018;226:113–23.

Sahoo S, Sahoo N, Biswal S, Mahapatra DK. Recent advances in indole derivatives with potent antimicrobial activity. Future Med Chem. 2021;13(11):987–1005.

Sahu B, Sharma AK, Pandey A. Design and synthesis of 2,3-substituted indole derivatives as antimicrobial agents. J Chem Pharm Res. 2018;10(4):321–9.

Saleem M, Ali MS, Hussain S. Synthesis and antibacterial activity of novel indole derivatives. J Chem Sci. 2019;131(12):1–11.

Samanta S, Rana S, Saha B. Structure-activity relationship of indole-based antibacterial agents. Med Chem Res. 2020;29(5):1123–36.

Saraswati J, Priya S, Kumar S. Design, synthesis, and characterization of indole derivatives for antimicrobial activity. Int J Res Pharm Chem. 2021;11(2):75–89.

Saxena P, Dwivedi S, Kumar A. Synthesis and biological activity of indole derivatives. Curr Med Chem. 2019;26(7):1236–50.

Sharma R, Gupta AK, Singh A. Recent developments in indole-based antimicrobial agents. Chem Rev. 2020;120(5):3124–50.

Sharma P, Jain R, Choudhary M. Synthesis and antibacterial evaluation of indole derivatives against resistant pathogens. Curr Top Med Chem. 2020;20(11):1005–19.

Shiroodi RK, Figueira J, Nakao S. Structure-activity relationship of indole derivatives as antimicrobials. Bioorg Med Chem. 2022;30(3):115123.

Singh M, Kaur P, Chadha S. Antimicrobial properties of synthetic indole derivatives. J Chem Pharm Res. 2018;10(8):11–23.

Singh SK, Kharb R, Chakarvarti AK. Structural diversity and therapeutic potential of indole derivatives. Bioorg Med Chem. 2021;36:115971.

Sirajuddin S, Suresh S, Anil KS. Synthesis, characterization, and evaluation of indole-based scaffolds. Med Chem Res. 2020;29(9):1812–26.

Sudhamani S, Rao PS, Devika R. Synthesis and antimicrobial evaluation of new indole derivatives. Bioorg Med Chem Lett. 2018;28(17):2687–91.

Sun J, Zhang Y, Nie Y, Guo Y. Antimicrobial activity of indole derivatives against multidrug-resistant pathogens. Int J Antimicrob Agents. 2022;59(2):106461.

Sun W, Choules MP, Berghuis AM. Multidrug-resistant bacterial infections: The need for new antibiotics. ACS Infect Dis. 2019;5(11):1682–91.

Tiwari R, Kumar P, Singh R. Advances in the development of indole-based antimicrobial agents. Future Med Chem. 2020;12(6):567–83.

Tomar V, Singh AK, Dubey S. Synthesis and biological evaluation of 2,3-disubstituted indole derivatives. Chem Biol Drug Des. 2018;91(1):71–83.

Tripathi A, Srivastava S, Gupta A. Design and synthesis of novel indole derivatives as antimicrobial agents. J Mol Struct. 2021;1222:128976.

Udupa S, Mehra S, Singh D. Synthesis and biological evaluation of indole derivatives as antimicrobial agents. Eur J Med Chem. 2020;184:111790.

Ujwala P, Mounika G, Lalitha D. Indole derivatives: Synthesis, characterization, and antimicrobial evaluation. J Pharm Res. 2019;13(2):123–32.

Yadav B, Singh R, Rana AK. Indole derivatives: Recent developments in antimicrobial activity. Med Chem Res. 2019;28(6):1149–65.

Zhang Y, Wang Y, Zeng D. Antibacterial activity of new indole derivatives. Eur J Med Chem. 2022;237:114301.